UNIVERSITE DE NICE - SOPHIA ANTIPOLIS

ECOLE DOCTORALE STIC
SCIENCES ET TECHNOLGIES DE L'INFORMATION ET DE LA COMMUNICATION

T H E S E

pour obtenir le grade de

Docteur ès Sciences

de l'Université Nice - Sophia Antipolis

Mention : AUTOMATIQUE, TRAITEMENT DU SIGNAL ET DES IMAGES

presentée et soutenue par

Stanley DURRLEMAN

Statistical models of currents for measuring the variability of anatomical curves, surfaces and their evolution

Thèse dirigée par
Nicholas AYACHE, Xavier PENNEC et Alain TROUVÉ
soutenue le 26 mars 2010

Jury :

Rapporteurs:	Polina GOLLAND	Professeur	MIT
	Jean-François MANGIN	Docteur	CEA - Neurospin
	David MUMFORD	Professeur	Brown University
Examinateurs:	Guido GERIG	Profeseur	University of Utah
	Stéphane MALLAT	Professeur	Ecole Polytechnique
Membre invité:	Laurent YOUNES	Professeur	Johns Hopkins University
Directeurs thèse:	Nicholas AYACHE	Docteur	INRIA - Sophia Antipolis
	Xavier PENNEC	Docteur	INRIA - Sophia Antipolis
	Alain TROUVÉ	Professeur	ENS Cachan

Part I

Currents for modeling curves and surfaces

Chapter 1

Curves and surfaces embedded in a metric space

Contents

In this chapter, we present mathematical objects called "currents", which are used as a model for general geometrical objects. In particular, we show that any sets of curves or surfaces may be embedded in the space of currents. This gives a non-parametric representation of such geometrical objects. These objects inherit from the *metric* defined in the space of currents: a geometric similarity measure between objects is provided, which does not assume any kind of point-correspondence between structures. The space of currents is a *vector space*: any set of geometrical structures may be decomposed into the union of several parts and each part may be weighted separately. This allows us to compare two sets of anatomical structures while adjusting the level of correspondence: correspondence between clusters of curves or between individual curves, for instance. This allows us to use any anatomical knowledge as prior without introducing arbitrary correspondences. The space of currents is also topologically *complete* and therefore allows us to process in the

same framework both discrete geometrical structures and continuous objects seen as the limit of sampled structures. This guarantees the robustness of the framework with respect to different sampling of the data.

Note: The first two sections may be read independently of the rest of the chapter. If you are not interested in the mathematical details of the modeling, you can switch to Chapter 2 after reading Section 1.2.

1.1 The giants on whose shoulders we stand

The idea of currents is deeply rooted into the theory of distributions, as set up by L. Schwartz in the 1940's [Schwartz 1966]. The distributions generalize the concept of function and measure on an open sub-space of $\mathbb{R}^d$. A distribution is characterized by its action on any infinitely differentiable (i.e. smooth) functions with compact support. A function f for instance, is completely determined by the collection of the integrals $\int f\phi$ for any smooth functions ϕ with compact support. Similarly, a measure μ is determined by the collection of $\int \phi d\mu$. More generally, a distribution is a continuous linear operator on the "test space" of the smooth functions with compact support. This idea of seeing an object (a distribution) via its action on a test space allowed to extend the concept of differentiability to non differentiable functions. In particular, this enables to state rigorously that the derivative of the Heaviside function is the Dirac delta distribution defined by $\delta_x(\phi) = \phi(x)$. The theory of distributions plays therefore a crucial role in the theory of partial differential equations and in Fourier analysis.

Distributions extend the concept of scalar functions. Currents is a similar construction but which extends the concept of differential forms on an open subset of $\mathbb{R}^d$ or on a smooth manifold. The theory of homological currents was developed by de Rham, as outlined in [Cartan 1970] and reported by Raoul Bott:

> *"When I met de Rham in 1949 at the Institute in Princeton he was lecturing on the Hodge theory in the context of his "currents". These are the natural extensions to manifolds of the distributions which had been introduced a few years earlier by Laurent Schwartz and of course it is only in this extended setting that both the de Rham theorem and the Hodge theory become especially complete."*

He named these objects "currents" by analogy with electromagnetism. For instance the Faraday's law of induction states that the intensity within a wire loop $\mathcal{C}$ induced by variations of a magnetic field $\mathbf{B}$ is proportional to the variations of the flux of this magnetic field through the surface S delimited by the wire (i.e. the boundary of S is $\mathcal{C}$): $\Phi(\mathbf{B}) = \int_S \mathbf{B}^t \mathbf{n} d\lambda$ (where $\mathbf{n}$ is the normal of the surface). This means that if we measure the intensity of the current within the wire (via the flux $\Phi(\mathbf{B})$) for every possible variations of the magnetic field (created by a moving magnet for instance), then we can retrieve the geometry of the wire. On the contrary, we can fix the magnetic field and move the wire $\mathcal{C}$ in the space. We can retrieve the value of the magnetic field by measuring the intensity of the Eddy currents in the wire for every possible motions of the wire. In this case, the wire is used to probe the magnetic field. In the first case, the magnetic field was used to probe

the geometry of the wire. These two examples show that the current $\mathcal{C}$ and the vector field $\mathbf{B}$ are two "dual" objects.

Initially, de Rham developed currents in order to find algebraic characterization of topological invariants on manifolds, which leads to his famous cohomology groups. However, currents quickly spread far beyond the field of algebraic and differential topology. In particular, they played a key role in the emergence of the "Geometric Measure Theory", pioneered by H. Federer [Federer 1969, Morgan 1987]. This theory tries to extend the measure theory (which leads to the integration theory of Lebesgue) to sub-manifolds, which are usually described by some parameterization (parametric curve or surface for instance). As explained by H. Federer, this should lead to a parameterization-free characterization of sub-manifolds:

> *"(...) one must abandon the idea of describing all the competing surfaces by continuous maps from a single predetermined parameter space. One should rather think of surfaces as m-dimensional mass distributions, with tangent m-vectors attached."*

This seminal vision leads to many theoretical developments and applications in various fields such as image processing and computational geometry. For instance, Wintgen and Zähle [Wintgen 1982] introduced particular currents called "Normal cycles" which generalize for singular objects the unit normal bundle of a smooth manifold. This tool was used to define curvature measures on a large class of geometric objects. Recent results of J.-M. Morvan and D. Cohen-Steiner [Cohen-Steiner 2003a, Cohen-Steiner 2003b] give an upper-bound of the error between the curvature measures of a polyhedron "close to" a sub-manifold and the curvature measures of the sub-manifold itself.

In 2005, J. Glaunès and M. Vaillant introduced the concept of currents in the field of Computational Anatomy [Glaunès 2005, Vaillant 2005]. Their purpose was to give a dissimilarity measure between meshes or polygonal curves which does not assume point-correspondence between structures, a key feature for comparing anatomical structures segmented automatically from Magnetic Resonance Images. They used this dissimilarity metric to drive the deformation of a source object (a set of curves or surfaces) to a target object. They proposed also to use the framework of reproducible kernel Hilbert space (RKHS) to give tractable formula of the metric as well as its derivatives.

In this chapter, we present the currents in the perspective of J. Glaunès' work with an emphasis on these two seminal ideas of currents: (1) currents model geometrical objects via their action on a test space of vector fields and (2) the modeling based on currents consider objects as a mass distribution without any kind of parameterization which would give a particular label to each point. Moreover, the topological properties of the space of currents enable to embed in a single framework smooth geometrical objects (on which the usual metric properties are naturally defined) and their discrete representation (the only objects to be accessible from a computational point of view).

1.2 An overview of currents in Computational Anatomy

The purpose of this section is to give a concise introductions of the currents without going into too much mathematical details. We introduce the concept of currents and the

main properties which are useful in the context of Computational Anatomy. The rigorous definitions and the proofs of the claimed properties will be given in the next section (see Section 1.3).

1.2.1 Currents: an object which integrates vector fields

Curves and surfaces tested on vector fields

As emphasized in the previous section, the main idea of currents is to probe shapes by vector fields. The word "shape" here is a generic word, which denotes a set of piecewise smooth curves or piecewise smooth surfaces (which will be modeled as rectifiable subsets of $\mathbb{R}^2$ and $\mathbb{R}^3$ in Section 1.3). As a consequence, a shape can be represented by an infinite set of oriented points: the set of all normals of the surfaces (resp. tangents of the curves). Such oriented points are called "momenta" in the sequel. In the discrete setting, shapes are given as meshes (resp. polygonal lines): the direction of the normals (resp. tangents) is constant over each mesh cell (reps. each segment).

Given ω a square integrable 3D vector field (a mapping from $\mathbb{R}^3$ to $\mathbb{R}^3$), any set of piecewise smooth surfaces S integrates ω thanks to the flux equation:

$$S(\omega) = \int_S \omega(x)^t n(x) d\lambda(x), \tag{1.2.1}$$

where $n(x)$ is the unit normal of the surface at point x and $d\lambda$ the Lebesgue measure on the surface. This equation computes the flux of the vector field ω through the surface S.

Similarly, any set of piecewise smooth curves L integrates a vector field ω thanks to the path-integral:

$$L(\omega) = \int_L \omega(x)^t \tau(x) d\lambda(x), \tag{1.2.2}$$

where τ is the tangent of the curve at point x and $d\lambda$ the Lebesgue measure on the curve. This equation computes the flux of the field of tangents through the equipotential surfaces of ω.

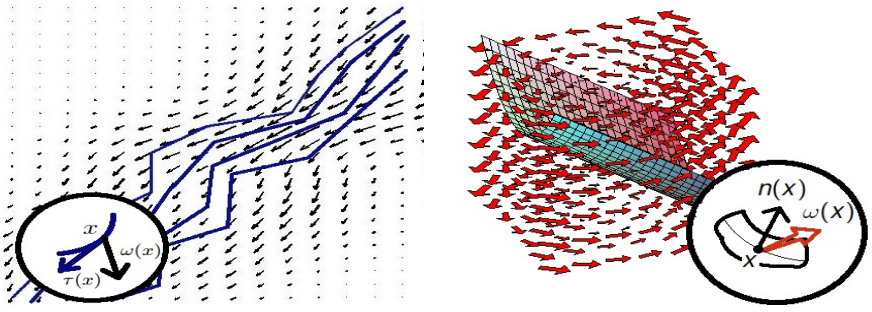

$$L(\omega) = \sum_{i=1\ldots4} \int_{L_i} \omega(x)^t \tau(x) d\lambda(x) \qquad S(\omega) = \int_S \omega(x)^t n(x) d\lambda(x)$$

Figure 1.1: In the framework of currents, curves and surfaces are tested on vector fields via the path-integral of the vector field along the curves (left) or via the flux-integral of the vector field through the surface (right). When we know the result of this operation for every vector fields possible, we get a characterization of the geometrical object.

The idea of currents is to characterize a shape by the collection of the real numbers $S(\omega)$ or $L(\omega)$ (given in Eq. (1.2.1) and (1.2.2) respectively) for all possible vector fields ω. For this purpose, we need to make precise the idea of 'all possible vector fields' by defining a proper test space of vector field: W.

Remark 1.1. We distinguish here between the case of curves and the case of surfaces. In Section 1.3, we will define a unifying framework for modeling curves, surfaces, unconnected point sets and volumes. In this framework, vector fields are replaced by differential forms. As shown in Appendix A, it appears that differential forms can be identified to vector fields when modeling curves in 2D or 3D and surfaces in 3D, thus leading to Eq. (1.2.1) and (1.2.2). These two particular cases are the one of most interest for the applications in Computational Anatomy. □

Test space of vector fields

We choose for the test space W the set of the convolutions between any square integrable vector fields and a smoothing kernel. Formally, W is defined as a Reproducing Kernel Hilbert Space (see Appendix B). The kernel plays the role of the transfer function of a low-pass filter. It enables to map every square integrable vector field to a smooth one. As a consequence, W cannot contain vector fields with too high spatial frequencies. In our applications, we will use a Gaussian kernel: $K^W(x,y) = \exp(-|x-y|^2/\lambda_W^2)\mathrm{Id}$ for any points (x,y), where Id stands for the identity map. In this case, the standard deviation λ_W is the typical scale at which the vector fields ω in W may vary spatially. As we shall see below, this kernel will allow us to control the metric on the space of currents and hence the measure of the distance between shapes.

In contrast to the usual space of square integrable vector fields (L^2), the RKHS of vector fields W have two important properties:

- W is the closed span of the vector fields of the form $\omega(x) = K^W(x,y)\beta$ for any fixed points y and vectors β (i.e. momentum (y,β)), meaning that any vector field ω can be written as an infinite linear combination of the basis elements $K^W(x,y)\beta$
- W is provided with an inner product which is defined on these basis vectors by

$$\left\langle K^W(.,x)\alpha, K^W(.,y)\beta \right\rangle_W = \alpha^t K^W(x,y)\beta \tag{1.2.3}$$

If we denote ω the vector field $K^W(.,y)\beta$ in Eq. (1.2.3), this equation can be written as:

$$\left\langle K^W(.,x)\alpha, \omega \right\rangle_W = \alpha^t \omega(x)\,. \tag{1.2.4}$$

Since the set of vector field of the form $K^W(.,y)\beta$ is dense in the RKHS W, this equation still holds for any vector fields ω in W (see Appendix B for details). It is called the "reproducing property".

The space of currents

The space of currents, denoted W^*, is the space of the continuous linear mappings from W to $\mathbb{R}$. Equations (1.2.1) and (1.2.2) show two examples of such mappings, thus making

any set of curves or surfaces a particular cases of currents. This means that shapes can be embedded into the space of currents. Each test space W defines a different embedding space W^*. As we shall see in the sequel, the parameter of the kernel λ_W will allow us to tune the metric properties of the embedding space of currents.

As a space of mappings, the space of currents is a *vector space*. Let T and T' be two surfaces (or two curves). The flux through the sum of the two currents $T+T'$ is equal to the sum of the flux through each surface: $(T+T')(\omega) = T(\omega) + T'(\omega)$. The sum in the space of currents is equivalent to the union of geometrical data. The opposite surface $-T$ in the space of current is the same surface but with opposite orientation (since the flux through the surface has then the opposite sign). A surface T may be weighted by a coefficient λ: $((\lambda T)(\omega) = \lambda(T(\omega))$. This allows us to give a relative weight to different pieces of surfaces, or to different surfaces within a set of surfaces.

Representation of currents in terms of vector fields

As a consequence of this definition, the Riesz representation theorem ensures that there is a linear mapping between the space of vector fields W and its dual space W^*, the space of currents (see Appendix B and Section 1.5 for more details). We denote this mapping $\mathcal{L}_W : W \longrightarrow W^*$. It is defined by:

$$\mathcal{L}_W(\omega)(\omega') = \langle \omega, \omega' \rangle_W \tag{1.2.5}$$

for all vector fields $(\omega, \omega') \in W$ (for $\omega \in W$, $\mathcal{L}_W(\omega)$ is a current, i.e. a mapping from W to $\mathbb{R}$). We call $\mathcal{L}_W(\omega)$ the dual representation of the vector field ω.

The dual representation of the basis vectors $K^W(x,.)\alpha$ are called the Dirac delta currents: $\delta_x^\alpha = \mathcal{L}_W(K^W(x,.)\alpha)$ (where the couple (x,α) is called a momentum). This shows that K^W is the Green function of the differential operator[1] $\mathcal{L}_W$. Combining Eq. (1.2.4) and Eq. (1.2.5), we get:

$$\delta_x^\alpha(\omega) = \left\langle K^W(x,.)\alpha, \omega \right\rangle_W = \alpha^t \omega(x)\,. \tag{1.2.6}$$

Decomposition of sub-manifolds as discrete currents

The previous equation shows that $\delta_x^\alpha(\omega) = \alpha^t\omega(x)$, which is the term within integrals in Eq. (1.2.1) and Eq. (1.2.2). A Dirac delta current may be interpreted therefore as an infinitesimal segment (or normal) α entirely concentrated at point x. Since W is a closed span of the vector fields $K^W(x,.)\alpha$, the space of currents is a closed span of the Dirac delta currents δ_x^α. This means that any currents may be decomposed into an *infinite* set of Dirac currents, like any piecewise smooth curves or surfaces is decomposed into the set of its tangents or normals.

In the discrete setting, the tangents of polygonal lines or normals of meshes are constant over the segments or the mesh cells. Therefore, one can approximate the set of tangents (resp. normals of a given segment (resp. mesh cell) by a single Dirac delta current δ_x^α

[1] An equivalent construction would consist of fixing a differential operator $\mathcal{L}_W$ and to denote K^W its Green function. However, we prefer here to have a closed form for the kernel instead of the differential operator. See Appendix B for more details.

where the momenta (x, α) is located at the center of mass the segment (resp. mesh cell) and the magnitude of the coefficient α encodes the length of the segment (resp. the are of the mesh cell). As a consequence the whole set of polygonal lines (resp. the meshes) may be approximated by a *finite* sum:

$$T \sim \sum_k \delta_{x_k}^{\alpha_k} . \tag{1.2.7}$$

Here we see again that the addition in the space of currents plays the role of the union of shapes: a surface mesh is seen as the union of its cells, each cells being approximated by a single Dirac delta current. We will prove in Section 1.3 that this approximation converges in the space of currents when the sampling of the discrete shapes becomes finer and finer. This shows that this modeling of curves and surfaces is weakly sensitive to the sampling of the geometrical objects. Moreover, the description in terms of the collection of momenta (i.e. oriented points) accounts only for local properties of the shapes. It makes the framework based on currents fully robust to topology changes or the change of connectivity between structures (like curves interruption or reconnection for instance). See illustrative example in Fig. 1.2.

The dual representation of this approximation in terms of vector field is given by (applying the linear map $\mathcal{L}_W^{-1}$ to Eq. (1.2.7) and combining with Eq. (1.2.5)):

$$\mathcal{L}_W^{-1}(T)(x) \sim \sum_k K^W(x, x_k)\alpha_k,$$

for any point $x \in \mathbb{R}^3$. This representation in terms of vector field is simply given by the convolution of every momentum (x, α) by the smoothing kernel K^W.

Thanks to this approximation, the integrals in Eq. (1.2.1) and Eq. (1.2.2) are replaced by their Riemann sums:

$$S(\omega) = \int_S \omega(x)^t n(x) d\lambda(x) \sim \sum_k \omega(x_k)^t n_k$$
$$L(\omega) = \int_L \omega(x)^t \tau(x) d\lambda(x) \sim \sum_k \omega(x_k)^t \tau_k$$

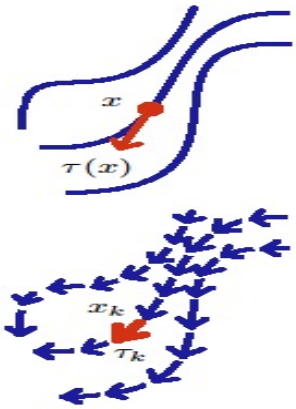

Figure 1.2: Both continuous and discrete shapes are handled in the same space of currents. In the continuous form, smooth curves are decomposed into the infinite set of their tangents. If curves are sampled, they can be approximated by a finite set of oriented points (called momenta) encoding each segment. The integral of a vector field ω on the smooth curve (i.e. a continuous current) is given as $L(\omega) = \int_L \omega(x)^t \tau(x) dx$. For the discrete approximation, this integral becomes a finite sum $L(\omega) = \sum_k \omega(x_k)^t \tau_k$. The discrete current converges to the continuous one as the sampling of the curves becomes finer and finer.

1.2.2 Correspondence-less distance between curves or surfaces

In this section, we introduce the metric on the space of currents. It will allow us to define a measure of the dissimilarity between two shapes without assuming point correspondences between structures.

The test space of vector field W is provided with an inner-product which satisfies Eq. (1.2.4). We can carry this inner-product to the space of current W^* via the linear map $\mathcal{L}_W$. The inner-product between two currents T and T' is then given as: $\langle T, T' \rangle_{W^*} = \left\langle \mathcal{L}_W^{-1}(T), \mathcal{L}_W^{-1}(T') \right\rangle_W$ where $\mathcal{L}_W^{-1}(T)$ denotes the vector field associated to T (if T is a discrete curve, $\mathcal{L}_W^{-1}(T)$ is the convolution of its tangents by the kernel). This makes $\mathcal{L}_W$ an isometric map between the space of vector field W and the space of currents W^*.

In W, the basis elements are the vector fields of the form $K^W(.,x)\alpha$. In W^*, the corresponding basis elements are the Dirac delta currents: $\delta_x^\alpha = \mathcal{L}_W^{-1}(K^W(.,x)\alpha)$. Therefore, the this inner-product between Dirac delta currents is given (thanks to Eq. (1.2.3)):

$$\begin{aligned} \left\langle \delta_x^\alpha, \delta_y^\beta \right\rangle_{W^*} &= \langle K(.,x)\alpha, K(.,y)\beta \rangle_W \\ &= \alpha^t K^W(x,y)\beta \,. \end{aligned} \tag{1.2.8}$$

By linearity, the inner product between two finite sets of Dirac currents $T = \sum_i \delta_{x_i}^{\alpha_i}$ and $T' = \sum_j \delta_{y_j}^{\beta_j}$ (which may model two discrete surfaces or two discrete curves) is given by:

$$\langle T, T' \rangle_{W^*} = \sum_i \sum_j \alpha_i^t K^W(x_i, y_j)\beta_j. \tag{1.2.9}$$

This equation gives *explicit* and *easily tractable* formula to compute the inner product between two discrete shapes. For continuous curves or surfaces, the sums in Eq. (1.2.9) are replaced by integrals.

We define now the distance between two shapes modeled as currents as the norm of their difference:

$$d(T, T') = \|T - T'\|_{W^*} = \sqrt{\langle T - T', T - T' \rangle_{W^*}}. \tag{1.2.10}$$

Combining with the definition of the map $\mathcal{L}_W$ in Eq. (1.2.5), we get:

$$\|T - T'\|_{W^*}^2 = (T - T')(\mathcal{L}_W^{-1}(T - T')). \tag{1.2.11}$$

In this equation, $T - T'$ is a current, namely an object which integrates vector fields, which is applied here to the vector field $\mathcal{L}_W^{-1}(T - T')$. Let us denote this vector field $\Delta(x) = \mathcal{L}_W^{-1}(T - T')(x)$. If T and T' are two curves whose tangents are denoted $\tau(x)$ and $\tau'(x)$ respectively, then:

$$\|T - T'\|_{W^*}^2 = \int_T \Delta(x)^t \tau(x) dx - \int_{T'} \Delta(x)^t \tau'(x) dx, \tag{1.2.12}$$

as illustrated in Fig. 1.3. If T and T' are discretized as finite sets of momenta ((x_p, α_p) and (y_q, β_q) respectively), then this squared norm becomes:

$$\|T - T'\|_{W^*}^2 = \sum_p \Delta(x_p)^t \alpha_p - \sum_q \Delta(y_q)^t \beta_q. \tag{1.2.13}$$

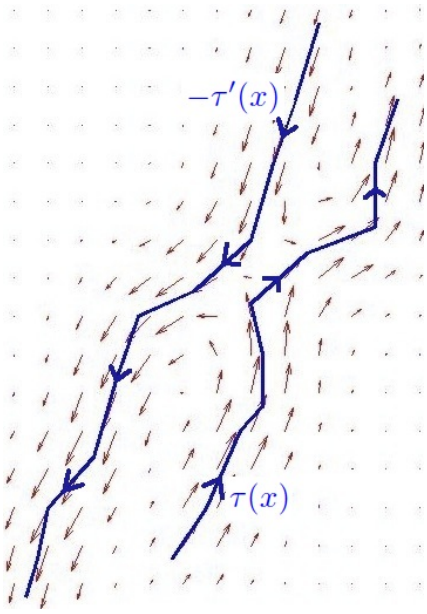

Figure 1.3: Distance between two curves L and L'. One builds the current $L - L'$ by inverting the orientation of L' and building the union of the tangents of both curves. The associated vector field $\Delta(x) = \mathcal{L}_W^{-1}(L - L')(x)$ is shown in red (i.e. the convolution of all the momenta of the L and $-L'$). The distance between both curves is given by the integration of this vector field along the curve L and the curve $-L'$: $\|L - L'\|^2 = \int_L \Delta(x)^t \tau(x) dx - \int_{L'} \Delta(x)^t \tau'(x) dx$. If the polygonal lines are approximated with a finite number of momenta, these integrals become finite sums over the segments of the lines.

The dense vector field $\Delta(x)$ is the vector field associated to the current $T - T'$. In case T and T' are given by the set of momenta $(x_p, \alpha_p)_{p=1\dots N}$ and $(y_q, \beta_q)_{q=1\dots N'}$, then the current $-T'$ is given by the momenta $(y_q, -\beta_q)$ (i.e. the orientation of the curve or the surface is changed) and eventually the current $T - T'$ is given by the union of all the momenta: $\{(x_p, \alpha_p)_{p=1\dots N}, (y_q, -\beta_q)_{q=1\dots N'}\}$. Its associated vector field is given by the convolution of these momenta by the kernel K^W, namely:

$$\Delta(x) = \mathcal{L}_W^{-1}(T - T')(x) = \sum_{p=1}^{N} K^W(x, x_p)\alpha_p - \sum_{q=1}^{N'} K^W(x, y_q)\beta_q \tag{1.2.14}$$

Combining this last equation with Eq. (1.2.13) leads to:

$$\|T - T'\|_{W^*}^2 = \sum_{p=1}^{N}\sum_{q=1}^{N} \alpha_p^t K^W(x_p, x_q)\alpha_q - 2\sum_{p=1}^{N}\sum_{q=1}^{N'} \alpha_p^t K^W(x_p, y_q)\beta_q + \sum_{p=1}^{N'}\sum_{q=1}^{N'} \beta_p^t K^W(y_p, y_q)\beta_q \tag{1.2.15}$$

This gives a closed form of the distance between two discrete curves or two discrete surfaces, which implies the kernel and every momenta representing the segments or the mesh cells of the shapes. Using Eq. (1.2.9), this last equation can be written as:

$$\|T - T'\|_{W^*}^2 = \|T\|_{W^*}^2 - 2\langle T, T'\rangle_{W^*} + \|T'\|_{W^*}^2 \tag{1.2.16}$$

which is the usual formula for computing the norm form inner-products.

We could have derived the closed form for the norm in Eq. (1.2.15) using only the usual identity in Eq. (1.2.16) and Eq. (1.2.9). However, we prefer to compute the distance $\|T - T'\|_{W^*}$ by introducing the vector field $\Delta(x)$, since this vector field has a geometrical interpretation. Indeed, we will show in Section 1.3 that this vector field is the one which achieves the supremum:

$$\sup_{\|\omega\|_W \neq 0} |T(\omega) - T'(\omega)| \,/\, \|\omega\|_W \,. \tag{1.2.17}$$

This means that if T and T' are two curves, the vector field $\Delta(x) = \mathcal{L}_W^{-1}(T - T')(x)$ is the one which maximizes the difference between the integral $T(\omega) = \int_T \omega(x)^t \tau(x) dx$ and the integral $T'(\omega) = \int_{T'} \omega(x)^t \tau'(x) dx$ over all the possible vector fields ω in the test space W. In some sense, this vector field is the one in W which best separates the two curves. Of course, if one changes the test space W, one changes this maximizing vector field and hence the measured distance between the curves. As illustrated in Fig 1.4, the highest the spatial frequencies of the vector fields in W, the more differences between both curves the maximizing vector field captures, the further the curves in the space of currents. The bandwidth of the vector fields in W is determined by the kernel (by the standard deviation λ_W for Gaussian kernel). This parameter can be tuned to set of "scale of noise" of shapes under which the geometrical details of shapes will be neglected, as illustrated in Fig. 1.5. Fig. 3.15 and 3.16 in Chapter 3 will also illustrate of the impact of the kernel on the distance between shapes.

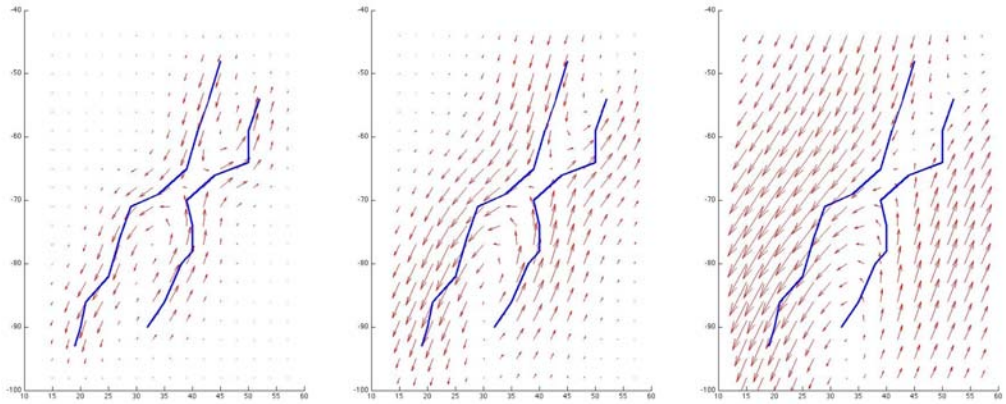

$\lambda_W = 5$ $\lambda_W = 10$ $\lambda_W = 20$

Figure 1.4: Impact of the kernel on the distance between two curves L and L' in blue. As in Fig. 1.3, the vector field associated to the current $L - L'$ is shown in red. This is the vector in the test space W which best separates the two curves. The result is shown for 3 different W: RKHS with Gaussian kernel and standard deviation: $\lambda_W = 5, 10$ and 20. For small λ_W, the vector field can vary fast enough, so that it can follows almost every small details of the curves and therefore almost perfectly interpolates between the directions of the curves: the two curves are almost orthogonal in the space of currents ($\arccos\left(\frac{|\langle L_1, L_2\rangle_{W^*}|}{\|L_1\|_{W^*}\|L_2\|_{W^*}}\right) = 85°$ for $\lambda_W = 5$). For large λ_W, the highest spatial frequencies are excluded from W: the vector field cannot adapt to the small-scale variations of the curves: the two curves become more and more aligned in the space of currents ($\arccos\left(\frac{|\langle L_1, L_2\rangle_{W^*}|}{\|L_1\|_{W^*}\|L_2\|_{W^*}}\right) = 65°$ for $\lambda_W = 10$ and $38°$ for $\lambda_W = 20$).

Figure 1.5: The choice of the kernel enables to adjust the metric on the space of currents. In particular, the rate of decay of the kernel (λ_W) determines the scale under which shape variations are considered as noise. On the left hand side, the bump is smoothed by the kernel and both lines are considered similar as currents. On the right-hand side the metric detects the bump as a shape dissimilarity. More precise discussion about the ability of the metric on currents to capture shape dissimilarity can be found in Section 3.5.2

1.2.3 Diffeomorphic deformations of currents

To include registration into the analysis of variability of anatomical structures, we need to define the deformation of currents in a way which is compatible with the usual geometric deformation of shapes.

Let ϕ be a diffeomorphism (a smooth deformation of the underlying 3D space, with smooth inverse) and S a surface. As a surface, S may be deformed by ϕ into $\phi(S)$ (the geometrical transportation of the points of S which still draw a surface). If we model S as a current, we define the push-forward current $\phi_* S$ such that the flux of any vector field ω through $\phi_* S$ is equal to the flux of ω through the transported surface $\phi(S)$. A change of variable within integrals of Eq. (1.2.1) and Eq. (1.2.2) leads to the definition: $\phi_* S(\omega) = S(\phi^* \omega)$ where the pull-back vector field $\phi^* \omega$ is equal to $|d_x \phi| \, (d_x \phi)^{-1} \omega(\phi(x))$ for surfaces and $d_x \phi^t \omega(\phi(x))$ for curves ($d_x \phi$ denotes the Jacobian matrix of ϕ and $|d_x \phi|$ its determinant). This action replaces for curves and surfaces the usual action on images: $(\phi_* I)(x) = I(\phi^{-1}(x))$. This is here slightly more complex since we do not transport points but tangents or normals (differential 1 and 2-forms, as will be explained in Section 1.3).

In practice, the push-forward action on the basis vectors is simply given by:

$$\phi_* \delta_x^\alpha = \delta_{\phi(x)}^{d_x \phi(\alpha)}, \tag{1.2.18}$$

in case α is a tangent of a curve. And

$$\phi_* \delta_x^{u \times v} = \delta_{\phi(x)}^{d_x \phi(u) \times d_x \phi(v)}, \tag{1.2.19}$$

in case $u \times v$ is the normal of a surface. One notices that by definition of the cross product, for any vector w, we have:

$$\begin{aligned} (d_x \phi(u) \times d_x \phi(v))^t w &= \det(d_x \phi(u), d_x \phi(v), w) \\ &= |d_x \phi| \det(u, v, d_x \phi^{-1}(w)) \\ &= |d_x \phi| \, (u \times v)^t d_x \phi^{-1}(w) = \left(|d_x \phi| \, d_x \phi^{-t}(u \times v) \right)^t w, \end{aligned} \tag{1.2.20}$$

where A^{-t} stands for $(A^{-1})^t$. Therefore, we have: $d_x \phi(u) \times d_x \phi(v) = |d_x \phi| \, d_x \phi^{-t}(u \times v)$.

And the deformation of an infinitesimal normal α is given by:

$$\phi_* \delta_x^\alpha = \delta_{\phi(x)}^{|d_x\phi| d_x\phi^{-t}\alpha}. \tag{1.2.21}$$

1.2.4 Currents: a solution to the (point)-correspondence issue

As emphasized in the introduction, this framework of currents has been chosen to measure dissimilarities between anatomical data. The anatomical structures extracted from MRI consist mostly of set of points which draw polygonal lines or surface meshes, as shown in Figure 1.6. These data may be seen as a hierarchical structure: points build curves or surfaces, individual curves or surfaces are gathered into clusters, a set of cluster builds complex multi-objects structures. At a certain level, these structures are labeled as anatomical structures, which have been proved to be stable features across the population. In the context of brain imaging for instance, some sulcal lines such as the Sylvian fissure can be found in almost every subject, whereas the individual points of the delineated Sylvian fissure are determined by the segmentation process and are not a stable anatomical feature.

It is crucial to account for this anatomical knowledge when comparing two sets of anatomical structure: the distance between these two sets should put into correspondence the clusters of points only at the anatomically relevant level. Comparing the data at a higher level leads to a less constrained distance, which will be less able to capture fine geometrical differences. It will also compare parts of the data which have different anatomical roles. Comparing the data at a lower level introduces correspondence without any anatomical reason. Such arbitrary constraints introduce bias in the analysis of the variability.

In the example of the fiber tracts of Fig. 1.6 (which will be explained with more details in Chapter 7), *individual* fibers extracted from diffusion images have never been shown to be a representation of some biological structures and have never been shown to be a stable feature across subjects. By contrast, *clusters* of these fibers draw fiber tracts which are considered as a representation, up to a certain precision, of the underlying white matter fiber bundles which connect two different functional areas of the cortex. In this example, we must compare pairs of fiber tracts and not pair of individual fibers.

The structure of vector space of the currents enables precisely to *adjust the level of correspondence* according to the anatomical knowledge. To compare the anatomical data of two subjects, one decomposes the data of each subject into the set of every tangent or normal. Let $T = \sum_i \delta_{x_i}^{\alpha_i}$ and $U = \sum_j \delta_{y_j}^{\beta_j}$ be the set of such oriented points for each subject. Then, we divide this set into clusters $\mathcal{C}_k$ according to the anatomical labels. Note that the number of points in a cluster may be very different for both subjects. By contrast, every subject is supposed to share the same anatomical description and, in particular, to have the same number of clusters. A cluster may be reduced to one single point if this point is considered as anatomically relevant, such as the anterior or the posterior commissure of the brain for instance. Then, a metric between the two data sets which account for the anatomical prior without introducing arbitrary correspondences can be written as:

$$\|T - U\|_{W^*}^2 = \sum_{\mathcal{C}_k} \lambda_k \left\| \left(\sum_{i \in \mathcal{C}_k} \delta_{x_i}^{\alpha_i} \right) - \left(\sum_{j \in \mathcal{C}_k} \delta_{y_j}^{\beta_j} \right) \right\|_{W^*}^2. \tag{1.2.22}$$

The two extreme cases are: (1) in absence of any anatomical knowledge, we compare the whole data-set as a single cluster $\left(\|T-U\|_{W^*} = \left\|\sum_i \delta_{x_i}^{\alpha_i} - \sum_{y_j}^{\beta_j}\right\|_{W^*}\right)$ and (2) each point has an anatomical label and we can assume correspondence between every pair of points (which requires that all the subjects have the same number of points) $\left(\|T-U\|_{W^*}^2 = \sum_k \lambda_k \left\|\delta_{x_i}^{\alpha_i} - \delta_{y_i}^{\beta_i}\right\|_{W^*}^2\right)$. The parameters λ_k enable to weight one anatomical structure with respect to the others. They can be used to normalize the total length or area of each anatomical structure for instance.

We remark that each cluster is considered as a *global* feature: a collection of infinitesimal tangents or normals. The topology of the shape is not taken into account. This makes the framework robust to curve interruption or reconnection for instance, a key feature for the comparison of fiber bundles as emphasized in Chapter 7. The distance on currents is also blind to the number of connected components of a mesh for instance.

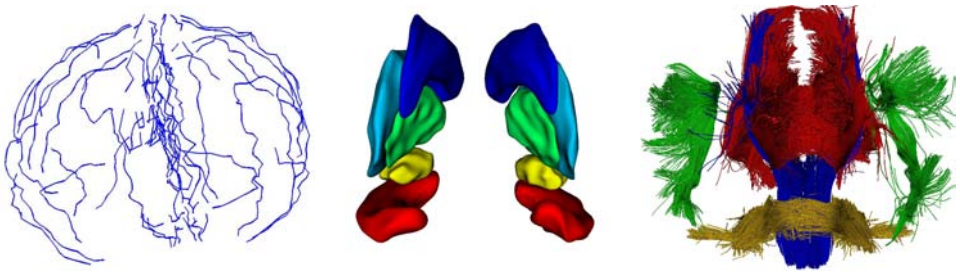

points	points	points
sulcal lines	meshes	individual fibers
set of sulci	set of meshes	fiber bundles
–	–	all fibers

Figure 1.6: Three examples of anatomical data-sets. Left: a set of sulcal lines. Each line is labeled (Sylvian fissure, central sulcus, etc.) and is supposed to be present in every subject in a normal population. Middle: set of 5 internal structures of the brain for each hemisphere. These structures are labeled (hippocampus, amygdala, etc..), whereas no point on this surface has been proved to play a particular anatomical role. Right: 5 white matter fiber bundles. Each bundle (set of thousands of curves) is labeled (corpus callosum, arcuate fasciculi, etc.) but not individual curves, whose number within a bundle may vary a lot across subjects. Only labeled structures are stable features across the population. Each of these structures must be compared as a global feature, without introducing arbitrary correspondence at a lower level (such as the individual curve level or point level, for instance). The framework based on currents allows us precisely to adjust the right level of correspondence according to the anatomical knowledge.

1.3 The mathematical construction of currents

In this section, we give the rigorous definitions of the concepts introduced in the previous one, prove the claimed properties and discuss the relevance of this model for anatomical data.

1.3.1 A unified model of geometrical data

The framework of currents has been presented in [Vaillant 2005] for modeling surfaces and in [Glaunès 2008] for modeling curves. A global framework for curves and surfaces has been introduced in [Glaunès 2005], along with objects called "measures" which model unstructured point-sets. In this thesis, we adopt a slightly different point of view and present a unified framework for modeling unstructured point sets, curves, surfaces, volumes and more generally any sub-manifold of dimension m in $\mathbb{R}^d$. This framework allows us also to account for possible scalar attributes on the geometrical structures. This feature could be used for image matching purposes for instance.

The key tool of the theory is the differential m-forms (see Appendix A). These objects generalize the concept of vector field (to a field of normals for instance, since the normal is the cross-product between two vectors). Therefore, they enable to embed in the same framework all kind of geometrical data.

The general definition of currents is given as a continuous linear map from a space of differential m-forms to $\mathbb{R}$, namely a linear form on differentiable m-forms. The parameter m determines the dimension of the sub-manifold which can be seen as a current. If $m = 0$ (differential 0-forms are scalar fields), a current is simply a distribution of Schwartz. For $m = 1$ and $m = 2$ we retrieve the case of curves and surfaces introduced in the previous section.

Definition 1.2 (currents)**.** *The space of m-currents is the dual space of the space of differential m-forms $\mathcal{C}^0(\mathbb{R}^d, (\Lambda^m\mathbb{R}^d)^*)$ (as in Definition A.6). The topological dual is meant in the same sense as for the Schwartz distributions [Schwartz 1966].*

Therefore, a m-current T maps every m-differential form ω to a real $T(\omega)$ such that:

$$T(\omega) \leq C_T \left\|\omega\right\|_\infty , \tag{1.3.1}$$

for a fixed constant C_T ($\|.\|_\infty$ denotes the supremum norm on $\mathcal{C}^0(\mathbb{R}^d, (\Lambda^m\mathbb{R}^d)^*)$ as in Definition A.6).

As a space of linear mappings, the space of m-currents is a vector space. For all currents T and T' and real λ, the map $(T+\lambda T')(\omega) = T(\omega)+\lambda T'(\omega)$ defines a m-current. Moreover, the space of current is provided with the following operator norm:

Definition 1.3 (mass-norm on currents)**.** *Let T be a m-current. The mass-norm of T is defined as the operator norm:*

$$M(T) = \sup_{\|\omega\|_\infty \leq 1} |T(\omega)| . \tag{1.3.2}$$

The main interest of currents is that sub-manifolds in $\mathbb{R}^d$ can be seen as currents. The following proposition shows that this is achieved via the integration of differential m-forms on sub-manifolds as introduced in Appendix A. In this proposition, we account for a possible image I which is drawn on the sub-manifold.

Proposition 1.4. *Let T be an oriented rectifiable sub-manifold of dimension m in $\mathbb{R}^d$ and I a scalar function on T, such that $\int_T |I(x)|\, d\lambda(x) < \infty$.*

Then, for any m-differential form ω in $\mathcal{C}^0(\mathbb{R}^d, (\Lambda^m \mathbb{R}^d)^*)$ the mapping:

$$T_I(\omega) = \int_T I\omega, \tag{1.3.3}$$

defines a m-current (the integral having the sense given in Definition A.7).

Proof. The mapping T_I defined in Eq. (1.3.3) is obviously linear with respect to ω. To make T_I a current, we must verify that this mapping is continuous. Using the notations of Definition A.7, we have:

$$\begin{aligned} |T_I(\omega)| &\leq \int_T |I(x)| \left| \omega(x) \left(\frac{u_1(x) \wedge \ldots \wedge u_m(x)}{|u_1(x) \wedge \ldots \wedge u_m(x)|} \right) \right| d\lambda(x) \\ &\leq \sup_{x \in \mathbb{R}^d} \sup_{|v_1 \wedge \ldots \wedge v_m| \leq 1} |\omega(x)(v_1 \wedge \ldots \wedge v_m)| \int_T |I(x)|\, d\lambda(x) \\ &\leq \|\omega\|_\infty \, \lambda(T_I), \end{aligned} \tag{1.3.4}$$

where $\lambda(T_I) = \int_T |I(x)|\, d\lambda(x)$ is the measure of the colored manifold T (if $I = 1$, $\lambda(T)$ is the length, area or volume of T according to the dimension m). This proves the continuity of the mapping. ■

Remark 1.5. In Proposition 1.4, the definition of the current T depends on the orientation of the sub-manifold. If we change the orientation of the sub-manifold T, then the integral has the opposite sign. Therefore the sub-manifold with the opposite orientation corresponds to the current $-T$. In other words, the sign of a current encodes an orientation. A sub-manifold vanishes in the space of currents if it is added to itself with opposite orientation. □

Now, we can show that the mass-norm introduced in Definition 1.3 is the generalization of the volume of a m-dimensional sub-manifold.

Proposition 1.6. *Let T be a bounded oriented rectifiable sub-manifold of dimension m in $\mathbb{R}^d$ and I a bounded non-negative scalar function on T. Proposition 1.4 makes the couple (T, I) a current denoted T_I. Then,*

$$M(T_I) = \lambda(T_I), \tag{1.3.5}$$

where $M(T_I)$ is the mass-norm of the current T_I (see Definition 1.3) and $\lambda(T_I) = \int_T I(x) d\lambda(x)$ the Lebesgue measure of the colored sub-manifold.

Proof. Equation (1.3.4) shows precisely that for all $\omega \in \mathcal{C}^0(\mathbb{R}^d, (\Lambda^m \mathbb{R}^d)^*)$:

$$|T_I(\omega)| \leq \|\omega\|_\infty \, \lambda(T_I) \tag{1.3.6}$$

This shows that $M(T_I) \leq \lambda(T_I)$. To show the equality, we construct a differential m-form ω which achieves the supremum in Equation (1.3.4).

Let $x \in T$ and $(u_1(x), \ldots, u_m(x))$ a positively oriented *orthonormal* basis of the tangent space of T at point x, defined almost everywhere. Then, we define the m-form $\omega(x)$ such that $\omega(x)(u_1(x) \wedge \ldots \wedge u_m(x)) = 1$ and $\omega(x)(\eta) = 0$ in every direction η orthogonal to $u_1(x) \wedge \ldots \wedge u_m(x)$ in $\Lambda^m \mathbb{R}^d$. Such a ω is build such that $T_I(\omega) = \int_T I(x) d\lambda(x)$. This collection of m-forms $\omega(x)$ (for $x \in T$) is therefore a good candidate to achieve the supremum. However, we still need to prove that it can be extended to continuous differential m-form defined on the whole space $\mathbb{R}^d$.

Since the sub-manifold is rectifiable, we can choose the orthonormal basis vectors $u_i(x)$ on each tangent space such that the map $x \to u_i(x)$ is continuous almost everywhere (we recall that the m-mutivector $\frac{u_1(x) \wedge \ldots \wedge u_m(x)}{|u_1(x) \wedge \ldots \wedge u_m(x)|}$ is invariant under a change of positively oriented basis in the tangent space of T at point x). This makes the mapping $x \to \omega(x)$ continuous almost everywhere on T. If T is continuously differentiable, then $x \to \omega(x)$ is continuous on T and it can be extended to a continuous differential m-form from $\mathbb{R}^d$ to $\Lambda^m \mathbb{R}^d$ which tends to zero at infinity. This constructed ω achieves the supremum. If T is only piecewise smooth, $x \to \omega$ is piecewise continuous. It can be approximated by a continuous differential m-form at any precision. This leads to the same supremum. ■

Remark 1.7. In this proof, we supposed that the bounded scalar function I is non-negative. This is not a strong limitation, since we can always shift this bounded function so that it is non-negative. In any case we have $M(T_I) \leq \lambda(T_I)$. If I is the linear, surface or volume mass density of the sub-manifold T, then $M(T_I)$ is the total mass of the manifold. This function I can also be used to give a weight to different parts of the shape T, for comparison purpose for instance. I can be also a gray-level image drawn on the manifold.

If $I = 1$ and if T is bounded (i.e. $\lambda(T) < \infty$), then

$$M(T) = \lambda(T). \tag{1.3.7}$$

In this case the mass of T is equal to the length, the area or the volume of the sub-manifold. If the sub-manifold is of dimension 0, the mass of T equals the number of points of T. □

1.3.2 Discretization in the space of currents

In this section, we show how polygonal lines, surface or volume meshes can be discretized in the space of currents: each face of the mesh can be approximated by a single Dirac delta current which represents an infinitesimal tangent or normal. Then, the approximation converges when the sampling of the meshes tend to zero, namely when the discrete mesh converges to a continuous curve or surface.

Before introducing the Dirac delta currents, we define general m-meshes in 3D. A 0-mesh is a finite set of points, a 1-mesh is set of segments, a 2-mesh is a set of triangles and a 3-mesh is a set of tetrahedrons.

Definition 1.8 (m-mesh)**.** *We define an oriented m-mesh in $\mathbb{R}^3$ as a finite collection of oriented m-dimensional simplexes ($0 \leq m \leq 3$). Each simplex is called the face or the cell of the m-mesh. It is denoted f_i for $i = 1, \ldots, N$ and N the total number of mesh cells. For*

each cell i, we denote $v_1^i, \dots, v_{m+1}^i$ its vertices and $c_i = \frac{1}{m+1}\sum_{k=1}^{m+1} v_k^i$ its center of mass. We define also $u_k^i = (v_{k+1}^i - v_0^i)/(m!)^{1/m}$, m vectors parallel to the edges of the simplex i (for $k = 1 \dots m$). We suppose that the order of the vertices have been chosen so that the basis $(u_k^i)_{k=1\dots m}$ has the same orientation as the mesh cell. Therefore, the m-multivector (see Appendix A) $u_1^i \wedge \dots \wedge u_m^i$ has the same sign as the orientation of the mesh cell and its norm equals the m-volume of the mesh cell (here m-volume denotes length, area or volume according to the dimension m).

In this definition, we limit the mesh cells to be simplexes, so that surface mesh cells must be triangles and volume mesh cells tetrahedrons. However, it is possible to extend this definition of arbitrary polyhedrons. In this case, we must define carefully a basis of vector space spanned by each polyhedron so that the m-multivector has the same orientation as the mesh cell and whose norm is equal to the m-volume of the cell. We also limit the definition of m-mesh to the 3D case. The definition could also be extended for arbitrary dimension, like the 4D dimension for modeling moving surfaces for instance.

Definition 1.9 (Dirac delta current)**.** *We denote by $\delta_x^{u_1\wedge\dots\wedge u_m}$ the linear form defined by:*

$$\forall \omega \in \mathcal{C}^0(\mathbb{R}^d, (\Lambda^m \mathbb{R}^d)^*), \quad \delta_x^{u_1\wedge\dots\wedge u_m}(\omega) = \omega(x)(u_1 \wedge \dots \wedge u_m)\,. \tag{1.3.8}$$

This mapping is obviously continuous and defines therefore a m-current.

Remark 1.10 (computing with Dirac delta currents)**.** We notice that this definition leads to the following rule:

$$a\delta_x^\alpha + \delta_x^\beta = \delta_x^{a\alpha} + \delta_x^\beta = \delta_x^{a\alpha+\beta}, \tag{1.3.9}$$

for any scalar a, m-multivectors α, β and point $x \in \mathbb{R}^d$. As a consequence, we will write linear combination of Dirac delta currents as $\sum_i \delta_{x_i}^{\alpha_i}$ where the upper-scripts include the weighting coefficients. In such sums, each point x_i are supposed to be distinct. □

According to Proposition 1.4, any bounded m-mesh with scalar attributes I is a current. In this setting, the mesh is considered as a piecewise $\mathcal{C}^1$ sub-manifold. However, from a computational point of view, a mesh is a discrete structure with a finite number of faces. In the following proposition, we show how a m-mesh can be approximated by a finite set of Dirac delta currents. The idea is simply to replace each cell of the mesh by a Dirac delta current: the entire m-volume of the cell is concentrated at its center of mass. This proposition shows also that currents can handle continuous and discrete structures in the same framework.

Proposition 1.11. *Let T be a m-mesh in the sense of Definition 1.8 and I a bounded scalar function defined on T. Thanks to Proposition 1.4, T_I is a current.*

We assume that the differential m-forms $\omega \in \mathcal{C}^0(\mathbb{R}^d, (\Lambda^m \mathbb{R}^d)^*)$ are C^1 and verify $\|\nabla_x \omega\|_\infty \leq C_\infty \|\omega\|_\infty$ for a fixed constant C_∞.

With the notations of Definition 1.8, let $I_i = \frac{1}{V_i}\int_{f_i} I(x)d\lambda(x)$ be the mean intensity of I over each face f_i of T, where $V_i = \left|u_1^i \wedge \dots \wedge u_m^i\right|$ is the m-volume of the face f_i. We define the current

$$\tilde{T}_I = \sum_i I_i \delta_{c_i}^{u_1^i\wedge\dots\wedge u_m^i}. \tag{1.3.10}$$

Then, the dissimilarity between T and $\tilde{T}$ in the space of currents is such that:

$$M(T_I - \tilde{T}_{\tilde{I}}) \leq C_\infty \|I\|_\infty M(T) \max_i \operatorname{diam}(f_i), \tag{1.3.11}$$

where $\operatorname{diam}(f_i)$ *denotes the diameter of the face* f_i.

Therefore, when the sampling of the mesh becomes finer ($\max_i \operatorname{diam}(f_i) \longrightarrow 0$*), the current* $\tilde{T}_{\tilde{I}}$ *converges to* T_I.

Proof. Let $\omega \in \mathcal{C}^0(\mathbb{R}^d, (\Lambda^m \mathbb{R}^d)^*)$. By definition of the Dirac delta currents, we have:

$$\tilde{T}_{\tilde{I}}(\omega) = \sum_i I_i \omega(c_i)(u_1^i \wedge \ldots \wedge u_m^i) = \sum_i \int_{f_i} I(x)\omega(c_i) \left(\frac{u_1^i \wedge \ldots \wedge u_m^i}{|u_1^i \wedge \ldots \wedge u_m^i|} \right) d\lambda(x)\,.$$

Thanks to Eq. (1.3.3), we have for T_I:

$$T_I(\omega) = \sum_{f_i} \int_{f_i} \omega(x) \left(\frac{u_1(x) \wedge \ldots \wedge u_m(x)}{|u_1(x) \wedge \ldots \wedge u_m(x)|} \right) I(x) d\lambda(x),$$

where $u_1(x), \ldots u_m(x)$ denotes a positively oriented basis of the tangent plane of T at point x, this integral being independent of the choice of the positively oriented basis. One notices now that every point on the flat face f_i shares the same tangent space, so that one can choose the same basis $u_1^i, \ldots, u_m^i$ at every point on the face. We have therefore:

$$\begin{aligned}
\left| T_I(\omega) - \tilde{T}_{\tilde{I}}(\omega) \right| &\leq \sum_i \int_{f_i} |I(x)| \left| \omega(x) \left(\frac{u_1^i \wedge \ldots \wedge u_m^i}{|u_1^i \wedge \ldots \wedge u_m^i|} \right) - \omega(c_i) \left(\frac{u_1^i \wedge \ldots \wedge u_m^i}{|u_1^i \wedge \ldots \wedge u_m^i|} \right) \right| \\
&\leq \|I\|_\infty \sum_i \int_{f_i} \underbrace{\sup_{|v_1 \wedge \ldots \wedge v_m| = 1} |(\omega(x) - \omega(c_i))(v_1 \wedge \ldots \wedge v_m)|}_{|\omega(x) - \omega(c_i)|_{(\Lambda^m \mathbb{R}^d)^*}} d\lambda(x) \\
&\leq \|I\|_\infty \|\nabla_x \omega\|_\infty \sum_i \int_{f_i} |x - c_i|\, d\lambda(x) \\
&\leq \|I\|_\infty C_\infty \|\omega\|_\infty (\max_i \operatorname{diam}(f_i)) \int_T d\lambda(x)\,.
\end{aligned} \tag{1.3.12}$$

According to Proposition 1.6, $\lambda(T) = M(T)$. This leads to:

$$\sup_{\|\omega\|_\infty \leq 1} \left| T_I(\omega) - \tilde{T}_{\tilde{I}}(\omega) \right| \leq C_\infty M(T) \|I\|_\infty \max_i \operatorname{diam}(f_i).$$

■

The following proposition shows that the discretization of a mesh in the space of currents preserves the mass-norm of the mesh.

Proposition 1.12. *Let T be a current of the form:*

$$T = \sum_{i=1}^N \delta_{x_i}^{\eta_i}, \tag{1.3.13}$$

for N distinct *points x_i and N m-multivectors η_i.*

Then the mass-norm of T is given as:

$$M(T) = \sum_{i=1}^{N} |\eta_i| \ . \tag{1.3.14}$$

Proof. For any m-differential form ω, we have:

$$T(\omega) = \sum_{i=1}^{N} \omega(x_i)(\eta_i) \, . \tag{1.3.15}$$

Therefore, we have that $T(\omega) \leq \sum\limits_{i=1}^{N} \sup\limits_{|u|\leq 1} |\omega(x_i)(u)| \, |\eta_i| \leq \|\omega\|_\infty \sum\limits_{i=1}^{N} |\eta_i|$. This implies that $M(T) \leq \sum_{i=1}^{N} |\eta_i|$.

To show the equality, we build a particular differential m-form ω which achieves the supremum in the previous equation (similarly as in the proof of Proposition 1.6). We choose a m-form $\omega(x_i)$ for every point x_i so that $\omega(x_i)(\eta_i / |\eta_i|) = 1$ in the direction of η_i and $\omega(x_i)(\eta_i^\perp) = 0$ in the directions $\eta_i^\perp$ orthogonal to η_i in $\Lambda^m \mathbb{R}^d$. Since, every points are distinct, we can interpolate between the points x_i so that the interpolated m-form is continuous and tends to 0 at infinity. For such a ω, $T(\omega) = \sum_{i=1}^{N} |\eta_i|$. ■

Corollary 1.13. *Let T be a m-mesh and I a non-negative bounded map on T. Let $\tilde{T}_I = \sum_{f_i} I_i \delta_{c_i}^{u_1^i \wedge \ldots \wedge u_m^i}$ be the discrete current which approximate T_I in the sense of Proposition 1.11. Then T_I and $\tilde{T}_I$ have the same mass-norm:*

$$M(T_I) = M(\tilde{T}_I) \, . \tag{1.3.16}$$

Proof. By application of Proposition 1.6, the mass-norm of T_I is equal to:

$$M(T_I) = \int_T I(x) d\lambda(x) = \sum_{f_i} \int_{f_i} I(x) d\lambda(x) = \sum_{f_i} V_i I_i = \sum_{f_i} I_i \left| u_1^i \wedge \ldots \wedge u_m^i \right| \, . \tag{1.3.17}$$

This last expression is precisely the mass-norm of $\tilde{T}_I$ by application of Proposition 1.12. ■

Remark 1.14 (Geometry and attributes: ambiguities?)**.** This discretization of colored currents in terms of Dirac delta currents may lead to some ambiguities. Indeed, let $I_i \delta_{x_i}^{u_m^i \wedge \ldots \wedge u_m^i}$ be an element of the discretization of a m-mesh. Due to the properties of the Dirac delta currents (see Eq. (1.3.9)), for any scalar a, we have:

$$I_i \delta_{x_i}^{u_m^i \wedge \ldots \wedge u_m^i} = \frac{I_i}{a} \delta_{x_i}^{a u_m^i \wedge \ldots \wedge u_m^i} . \tag{1.3.18}$$

This means that a change of attribute (I_i becomes I_i/a) may balance a scaling of the mesh cell. In other words, the discretization of two meshes with different size of mesh cells could be undistinguishable if the change of size is overcome by a change of attributes. However, such meshes, seen as continuous currents, are distinct. This is a bad effect of the discretization.

In this thesis, we will not use scalar attributes. As a consequence, the magnitude of the momenta of the discrete approximation of a m-mesh encodes the area of the mesh cells.

The possible ambiguity between geometry and scalar attributes may be a problem for using currents to match grey-level images. During registration of discretized images with

currents, the algorithm may tend to change the size of the voxel to accommodate to the change of intensity. Although we believe that image registration can be performed in this framework, one must design specific solution to this problem. A re-meshing of the image during registration could be investigated, for instance. □

1.3.3 Action of the group of diffeomorphism on the space of currents

In this section, we define the deformation of a general current T so that, when T is the current associated to a sub-manifold, the deformation of the current (denoted $\phi_* T$) corresponds to the deformed sub-manifold $\phi(T)$.

If T is an oriented rectifiable sub-manifold of dimension m in $\mathbb{R}^d$ and ϕ is diffeomorphism of $\mathbb{R}^d$, then $\phi(T)$ remains an oriented rectifiable sub-manifold (with the same regularity as T). If I is a scalar map on the sub-manifold T, then $I \circ \phi^{-1}$ is a map on $\phi(T)$: the attribute of $\phi(T)$ at point $\phi(x)$ is the same as the attribute of T at point x: attributes are not affected by the deformation. Therefore, Proposition 1.4 makes the couple $(\phi(T), I \circ \phi^{-1})$ a colored current. We denote this current $\phi_* T_{I \circ \phi^{-1}}$. This current maps every differential m-forms $\omega \in \mathcal{C}^0(\mathbb{R}^d, (\Lambda^m \mathbb{R}^d))$ to $\phi_* T_{I \circ \phi^{-1}}(\omega) = \int_{\phi(T)} (I \circ \phi^{-1}) \omega$. We can now apply the change of variable formula as in Eq. (A.3.8) to this integral. This gives:

$$\phi_* T_{I \circ \phi^{-1}}(\omega) = \int_{\phi(T)} I \circ \phi^{-1} \omega = \int_T I \phi^* \omega = T_I(\phi^* \omega)\,, \tag{1.3.19}$$

where T_I in the last term is the colored current associated to the sub-manifold T and the map I. ϕ^* denotes the pullback action on differential m-forms as in Definition A.11. The equality: $\phi_* T_{I \circ \phi^{-1}}(\omega) = T_I(\phi^* \omega)$ still makes sense even if T_I is not the current associated to a sub-manifold but a more general current. This allows us to define the action a diffeomorphism ϕ on any current T as follows:

Definition 1.15 (push-forward action on currents)**.** *Let T be a m-current in $\mathbb{R}^d$ and ϕ a diffeomorphism of $\mathbb{R}^d$ such that $\sup_{x \in \mathbb{R}^d} |d_x \phi| < \infty$. The push-forward action of ϕ on T is defined by:*

$$\phi_* T(\omega) = T(\phi^* \omega) \tag{1.3.20}$$

for all differential m-forms $\omega \in \mathcal{C}^0(\mathbb{R}^d, (\Lambda^m \mathbb{R}^d)^*)$.

We can easily check that this defines an action of the group of diffeomorphism on the space of currents: $(\phi \circ \psi)_* T = \phi_*(\psi_* T)$, since the pullback is also an action as mentioned in Appendix A. Moreover, the action is linear:

$$\phi_*(T + \lambda T') = \phi_* T + \lambda \phi_* T', \tag{1.3.21}$$

for any currents T and T' and any real numbers λ.

Proposition 1.16. *If T is a sub-manifold of $\mathbb{R}^d$ and I a map on T such that $\int_T |I(x)|\, d\lambda(x) < \infty$, then the sub-manifold $\phi(T)$ associated to the map $I \circ \phi^{-1}$ is a current. This current is equal to $\phi_*(T_{I \circ \phi^{-1}})$.*

Proof. This is exactly what we proved in Eq. (1.3.19). ■

Now, we can apply Definition 1.15 on Dirac delta currents:

Proposition 1.17. *Let ϕ be a diffeomorphism of $\mathbb{R}^d$. The deformation of a m-Dirac delta current is given by:*

$$\phi_* \left(\delta_x^{u_1 \wedge \ldots \wedge u_m}\right) = \delta_{\phi(x)}^{(d_x\phi(u_1)) \wedge \ldots \wedge (d_x\phi(u_m))} . \tag{1.3.22}$$

Proof. For any differential m-form ω, we have by definition of the push-forward action on currents:

$$\begin{aligned} \phi_* \left(\delta_x^{u_1 \wedge \ldots \wedge u_m}\right)(\omega) &= \delta_x^{u_1 \wedge \ldots \wedge u_m}(\phi^*\omega) \\ &= \phi^*\omega(x)\left(u_1 \wedge \ldots \wedge u_m\right) \\ &= \omega(\phi(x))\left(d_x\phi(u_1) \wedge \ldots \wedge d_x\phi(u_m)\right) \\ &= \delta_{\phi(x)}^{d_x\phi(u_1) \wedge \ldots \wedge d_x\phi(u_m)}(\omega) \end{aligned} \tag{1.3.23}$$

which gives the expected result. ■

1.4 Particular cases of practical interest

In the applications, we are mainly interested in modeling unstructured point-sets in 2D or 3D ($m = 0, d = 2, 3$), curves in 2D or 3D ($m = 1$, $d = 2, 3$), surfaces in 3D ($m = 2$, $d = 3$) and volumes in 3D ($m = 3$, $d = 3$). These cases, all of great practical interest, fall into one of these 4 categories: they are of dimension 0 ($m = 0$), co-dimension 0 ($d - m = 0$), dimension 1 ($m = 1$) or co-dimension 1 ($d - m = 1$). In these cases, the m-forms can be represented by scalar fields (dimension or co-dimension 0) or vector fields (dimension or co-dimension 1), as shown in Appendix A.

In this section, we apply the construction of the previous section to these particular cases. We retrieve then the properties claimed in Section 1.2.

1.4.1 Unstructured point sets

The 0-forms are constant mappings and differential 0-forms map every point $x \in \mathbb{R}^d$ to a scalar $\omega(x)$. A differential 0-form is therefore a scalar field.

Let A be a discrete set of points $\{x_i\}$ associated to some scalar I_i such that $\int_A I(x)d\lambda(x) = \sum_{i \in A} I_i < \infty$. We recall that for sub-manifold of dimension 0, the measure $d\lambda = \sum_{x \in A} \delta_x$ counts the number of elements in A. Therefore, A may be modeled as the 0-current via :

$$A_I(\omega) = \int_A I(x)\omega(x)d\lambda(x) = \sum_i I_i\omega(x_i). \tag{1.4.1}$$

This shows that the sub-manifolds of dimension 0 are directly given as a sum of Dirac delta currents:

$$A = \sum_i \delta_{x_i}^{I_i} \tag{1.4.2}$$

Let ϕ be a diffeomorphism of $\mathbb{R}^d$. The push-forward action of ϕ on the 0-current A is given as:

$$\phi_* A = \delta_{\phi(x_i)}^{I_i}. \tag{1.4.3}$$

In these equations, we notice that the diffeomorphism ϕ just moves the point of A while keeping unchanged the attributes I_i. These coefficients are seen as intrinsic weights of each points, or probabilities if $\sum_i I_i = 1$.

1.4.2 Curves in any dimension

A 1-form is a linear form on $\mathbb{R}^d$ (i.e. linear mapping from $\mathbb{R}^d$ to $\mathbb{R}$). Thanks to the Riesz theorem, any linear form may be represented by the inner product: $\omega(u) = \overline{\omega}^t u$ for a constant vector $\overline{\omega} \in \mathbb{R}^d$. A differential m-form may be represented therefore by a vector field $\overline{\omega}(x)$ such that for all points $x \in \mathbb{R}^d$ and all vectors $u \in \mathbb{R}^d$, $\omega(x)(u) = \overline{\omega}(x)^t u$. In the sequel, we denote ω both the 1-form $\omega(x)$ and the vector field $\overline{\omega}(x)$.

Let L be a set of piecewise continuous curves and $I(x)$ an integrable scalar map on these curves. L may be seen as a 1-current via:

$$L_I(\omega) = \int_L I(x)\omega(x)^t \tau(x) d\lambda(x) \tag{1.4.4}$$

for every vector field ω, where $\tau(x)$ is the unit tangent vector of the curves L at point x. We recall that $d\lambda$ denotes the Lebesgue measure on the curves, so that $\int_L d\lambda(x)$ equals the total length of the curves.

If the curves L are polygonal lines (whose segments are denoted s_i), they can be approximated as

$$\tilde{L}_I = \sum_{s_i} \delta_{c_i}^{I_i \tau_i}, \tag{1.4.5}$$

where τ_i is the oriented segment s_i and $I_i = \frac{1}{|\tau_i|} \int_{s_i} I(x) d\lambda(x)$ the mean attribute over the segment s_i. Its action on a vector field ω is given by: $\tilde{L}_I(\omega) = \sum_i I_i \omega(c_i)^t \tau_i$.

If ϕ is a diffeomorphism of $\mathbb{R}^d$, then the deformed current $\phi_* L_{I \circ \phi^{-1}}$ is given by

$$\begin{aligned} \phi_* L_{I\circ\phi^{-1}}(\omega) = L_I(\phi^*\omega) &= \int_L I(x)\omega(\phi(x))^t (d_x\phi)\tau(x) d\lambda(x) \\ &= \int_L I(x) \left(d_x\phi^t \omega(\phi(x))\right)^t \tau(x) d\lambda(x)\,. \end{aligned} \tag{1.4.6}$$

In the discrete case, we have:

$$\phi_* \left(\sum_i I_i \delta_{c_i}^{\alpha_i} \right) = \sum_i I_i \delta_{c_i}^{d_{c_i}\phi(\alpha_i)}\,. \tag{1.4.7}$$

In this equation, we remark that the density $I(x)$ remains unchanged during the deformation and that the tangents of the curves are deformed according to the Jacobian of the deformation ϕ.

1.4.3 Surfaces in 3D

As shown in Appendix A, the space of 2-forms in dimension 3 is of dimension 3. Each 2-form ω is associated isometrically to a 3D-vector $\overline{\omega}$, such that $\omega(u,v) = \det(u,v,\overline{\omega}) = \overline{\omega}^t(u \times v)$ for all vectors (u,v), where $\times$ denotes the cross-product in $\mathbb{R}^3$. Therefore, a differential 2-form may be represented by a vector field $\overline{\omega}(x)$: $\omega(x)(u,v) = \overline{\omega}(x)^t (u \times v)$. In the sequel, $\omega(x)$ denotes both the differential 2-form and its associated vector field.

Let S be a set of piecewise continuous surfaces and I an integrable scalar map on S. S may be seen as a 2-current via:

$$S_I(\omega) = \int_S I(x)\omega(x)^t \left(u(x) \times v(x)\right) d\lambda(x) = \int_S I(x)\omega(x)^t n(x) d\lambda(x) \tag{1.4.8}$$

for every vector field ω, where $n(x) = u(x) \times v(x)$ is the unit normal vector of the surfaces S at point x ($(u(x), v(x))$ being an orthonormal basis of the tangent plane of the surface S at point x).

If the surfaces S are surface meshes (whose mesh cells are denoted f_i), they can be approximated as

$$\tilde{S}_I = \sum_{f_i} \delta_{c_i}^{I_i n_i}, \tag{1.4.9}$$

where $n_i = u_1^i \times u_2^i$ (in the sense of Definition 1.8) is the oriented normal of face f_i whose norm is equal to the surface of f_i, $I_i = \frac{1}{|n_i|}\int_{f_i} I(x)d\lambda(x)$ the mean attribute over the face f_i and c_i the center of mass of the face f_i. Its action on a vector field ω is given by: $\tilde{S}_I(\omega) = \sum_i I_i \omega(c_i)^t n_i$. Note that in this equation we write $\delta_x^{u\wedge v}$ for the 2-multivector $u \wedge v$ in 3D as $\delta_x^{u\times v}$ where $u \times v$ is the 3D-vector which characterizes $u \wedge v$ (see Appendix A). This notation, however, may be misleading since the dimension of the current ($m = 2$) is no more visible in this expression (see Remark 1.18).

If ϕ is a diffeomorphism of $\mathbb{R}^d$, then the deformed current $\phi_* S_{I\circ\phi^{-1}}$ is given by

$$\begin{aligned} \phi_* S_{I\circ\phi^{-1}}(\omega) = S_I(\phi^*\omega) &= \int_S I(x)\omega(\phi(x))^t \left(d_x\phi u(x) \times d_x\phi v(x)\right) d\lambda(x) \\ &= \int_S I(x) \left(|d_x\phi|\, d_x\phi^{-1}\omega(\phi(x))\right)^t n(x) d\lambda(x). \end{aligned} \tag{1.4.10}$$

In the discrete case, we have:

$$\phi_* \left(\sum_i I_i \delta_{c_i}^{n_i} \right) = \sum_i I_i \delta_{c_i}^{\left|d_{c_i}\phi\right| d_{c_i}\phi^{-t} n_i}. \tag{1.4.11}$$

1.4.4 Volumes in any dimension

As shown in Appendix A, all d-forms in dimension d are proportional to the determinant. This means that every d-form in $\mathbb{R}^d$ has the form: $\omega(u_1 \wedge \ldots \wedge u_d) = \overline{\omega} \det(u_1, \ldots, u_d)$, where $\overline{\omega}$ is a scalar which characterizes the d-form ω. As a consequence, a differential d-form in $\mathbb{R}^d$ is characterized by a scalar field $\overline{\omega}(x)$ such that $\omega(x)(u, v, w) = \overline{\omega}(x) \det(u, v, w)$. In the sequel, $\omega(x)$ denotes both the differential d-form and its associated scalar field.

Let V be a set of continuous volumes and I an integrable scalar map on V. V may be seen as a 3-current via:

$$V_I(\omega) = \int_V I(x)\omega(x) \det(u_1(x), \ldots, u_d(x)) d\lambda(x) = \int_V \omega(x) d\lambda(x) \tag{1.4.12}$$

for every scalar field ω, where $u_1(x), \ldots, u_d(x)$ is a positively oriented orthonormal basis of $\mathbb{R}^d$ and as such $\det(u_1(x), \ldots, u_d(x)) = 1$.

If the volumes V are volume meshes in 3D (whose mesh cells are denoted f_i), they can be approximated as

$$\tilde{V}_I = \sum_{f_i} \delta_{c_i}^{I_i v_i} \tag{1.4.13}$$

where c_i denotes the center of the polyhedron f_i, v_i the volume of the polyhedron f_i and $I_i = \frac{1}{v_i}\int_{f_i} I(x)d\lambda(x)$ the mean intensity in the volume f_i. The action of this 3-current on a vector field ω is given by: $\tilde{V}_I(\omega) = \sum_i I_i v_i \omega(c_i)$.

If ϕ is a diffeomorphism of $\mathbb{R}^d$, then the deformed current $\phi_* V_{I\circ\phi^{-1}}$ is given by

$$\begin{aligned}\phi_* V_{I\circ\phi^{-1}}(\omega) = V_I(\phi^*\omega) &= \int_V I(x)\omega(\phi(x))\det(d_x\phi u_1(x),\ldots,d_x\phi u_d(x))d\lambda(x)\\ &= \int_V I(x)\omega(\phi(x))\,|d_x\phi|\,d\lambda(x)\,.\end{aligned} \tag{1.4.14}$$

We notice in particular that this action is different from the one on the scalar field associated to a 0-current due to the Jacobian $|d_x\phi|$.

In the discrete case, we have:

$$\phi_*\left(\sum_i I_i\delta_{x_i}^{v_i}\right) = \sum_i I_i\delta_{x_i}^{|d_{c_i}\phi|v_i}\,. \tag{1.4.15}$$

Note that, like the 0-currents, 3-currents are build on scalar fields. But for 3-currents, the action of a diffeomorphism takes into account the deformation of the geometry of the volumes. The volume v_i is changed according to the determinant of the Jacobian of the deformation.

Remark 1.18 (On the notations)**.** The notation of Dirac Delta current δ_x^α in this context is misleading since it may denote 0-,1-,2- and 3-currents. Indeed α may be a scalar, a vector, the vector associated to a 2-multivector or the scalar associated to a 3-multivector. In particular, the reader has to keep in mind that the upper-script in this notation **has a unit**! For the 0-current δ_x^α, α is a pure scalar (without any unit) and it is not affected by the deformation. On the contrary, if δ_x^α denotes a 3-current, then the scalar α is the measure of a volume which is mutliplied by the Jacobian of the deformation when the current moves in space. Similarly, a vector α in the notation δ_x^α has the unit of a length for a 1-current and the unit of a surface for a 2-current. It is deformed by a diffeomorphism according to its dimension. □

Remark 1.19 (Take care of the dimension!)**.** In this section, we introduced m-currents for modeling sub-manifolds of dimension m in $\mathbb{R}^3$. However, it is possible to consider a manifold of dimension m as a collection of manifolds of lower dimension. For instance, curves, surfaces or volumes can be all considered as continuous point sets. Similarly, a surface may be described as dense collection of curves (a moving curve which sweeps the surface). In this example, the surface may be modeled as a single 2-current or as a sum of 1-currents. One must be aware that these two currents are *not* equivalent. They do not have the same geometrical properties. This is particularly visible when considering the deformation of the currents. The action of a diffeomorphism on the collection of curves deforms the surface in the direction of the curves only, whereas the action on the 2-current affects also the surface in the direction orthogonal to the curves.

Similarly, let $\mathcal{C}$ be a polygonal line $\{x_1,\ldots,x_n\}$. Modeled as a 1-current this curve is represented by $C_1 = \sum_{i=1}^{n-1}\delta_{x_i}^{x_{i+1}-x_i}$. Modeled as a collection of points, the curve is represented by the 0-current: $C_0 = \sum_{i=0}^{n}\delta_{x_i}$. Let ϕ be a diffeomorphism of the space.

The deformed 1-current is given by: $\phi_* C_1 = \sum_{i=1}^{n-1} \delta_{\phi(x_i)}^{d_{x_i}\phi(x_{i+1}-x_i)}$, whereas the deformed 0 current is written as: $\phi_* C_0 = \sum_{i=1}^{n} \delta_{\phi(x_i)}$. Only the first current $\phi_* C_1$ is the discretization of the deformed curve $\phi(\mathcal{C})$ (in particular the mass-norm of $\phi_* C_1$ is equal to the length of $\phi(\mathcal{C})$). By contrast, $\phi_* C_0$ does not take the tangential information into account. $\mathcal{C}$ and *the set of points on* $\mathcal{C}$ are two different objects: the one is of dimension 1, the other of dimension 0. As a conclusion, any current is associated to a particular dimension m. And there is no simple way to describe a m-current as a collection of $(m-1)$-currents while preserving the same geometrical properties.

In practice, the segmentation of an anatomical surfaces or volumes may be given as an unstructured point-set. In absence of surface or volume mesh, one has no other choice than modeling this set of points as a 0-current. One must be aware, however, that building a surface or a volume mesh from this point set would reconstruct the geometry of the anatomical structure and lead eventually to different measures of similarity, which would account for this richer geometrical information. □

Remark 1.20 (Why using m-forms instead of scalar/vector fields?)**.** There are some cases of practical interest which are not modeled with differential m-forms of dimension or co-dimension 0 or 1. For instance, one may be interested in the temporal evolution of a curve in 3D. This can be seen as a tubular surface ($m = 2$) in a 4D space ($d = 4$). In this case, the representation in terms of vector field is no more possible, whereas the framework based on currents still applies. However, from a computational point of view, the algorithms presented in this thesis take advantage of the representation in terms of vector/scalar fields. Dealing with other cases would require to develop new algorithms. □

1.5 The space of currents as a RKHS

1.5.1 Why the mass-norm is not adapted to measure shape dissimilarity

In the previous section, we introduced the mass-norm of a current. However, the following proposition shows that this norm cannot be used in practice for measuring shape dissimilarities. Indeed, this measure is insensitive to the relative distance between two sub-manifolds, as long as they do not intersect.

Proposition 1.21. *Let T and T' be two smooth compact sub-manifolds with disjoint supports. Then*

$$M(T - T') = M(T) + M(T')\,. \tag{1.5.1}$$

Let T and T' be two finite sums of Dirac delta currents located at different points. Then,

$$M(T - T') = M(T) + M(T')\,. \tag{1.5.2}$$

Proof. The proof is a generalization of the proofs of Proposition 1.6 and Proposition 1.12 and relies on the same idea. The triangle inequality states that $M(T - T') = \sup_{\|\omega\|_\infty \leq 1} |T(\omega) - T'(\omega)| \leq M(T) + M(T')$ in both cases. To show the equality, one finds a particular ω which enables to achieve the supremum. We focus on the case of sub-manifolds

since the case of Dirac currents is direct consequence of Proposition 1.12. For any x in T and T', we choose the m-form $\omega(x)$ such that $\omega(x)(u_1(x) \wedge \ldots \wedge u_m(x)) = |u_1(x) \wedge \ldots \wedge u_m(x)|$ and 0 in the directions orthogonal to $u_1(x) \wedge \ldots \wedge u_m(x)$ in $\Lambda^m \mathbb{R}^d$, where $u_i(x)$ denotes a basis of the tangent plane of T at point x. Since the sub-manifolds are smooth, we can choose basis vectors $u_i(x)$ which varies continuously on each sub-manifold, thus making $\omega(x)$ continuous on T and T'. Now, since T and T' are disjoint, we can interpolate continuously the values of $\omega(x)$ in-between T and T'. Since the sub-manifolds are compact, we can also make $\omega(x)$ tend to 0 at infinity. Therefore, this constructed ω belongs to $\mathcal{C}^0(\mathbb{R}^d, (\Lambda^m \mathbb{R}^d)^*)$ and achieves the supremum in the definition of the norm. ■

Remark 1.22. There is no contradiction between this proposition and Proposition 1.11 since the support of the discretized current $\tilde{T}$ is included into the support of the original current T. □

Remark 1.23 (support of a current)**.** This Proposition can be expressed in a more general form for any currents T and T' with disjoint supports. However, for the sake of simplicity, we do not define the support of a current and focus on two particular cases: sub-manifolds and Dirac delta currents. However, the definition of the support of a distribution [Schwartz 1966] extends straightforwardly to currents. □

Let us take two Dirac currents δ_x^α and δ_y^α which model two small mesh cells (infinitesimal surface for instance) with the same orientation but located at two distinct points x and y. The dissimilarity between these two currents is equal to $M(\delta_x^\alpha - \delta_y^\alpha) = 2\,|\alpha|$, thus meaning that the distance between both structures is constant as long as $x \neq y$. But once $x = y$, then $M(\delta_x^\alpha - \delta_y^\alpha) = 0$. This shows that the metric M is blind to shape dissimilarities until the two shapes are perfectly aligned! As a consequence, it is not possible to use this metric to drive the registration of one shape onto another. Moreover, the discontinuous behavior of the metric with respect to the positions x and y prevents us from using the mass-norm from a numerical point of view.

The main problem is that the mass-norm is the dual norm for the supremum norm for continuous differential m-form. The key argument in the proofs of Propositions 1.6, 1.12 and 1.21 is that we can always find a differential m-form ω which continuously interpolates between $\omega(x) = \alpha$ and $\omega(y) = -\alpha$ for two distinct points x and y. If we impose some constraints on the variations of ω, then it may not be possible to interpolate with bounded variations between arbitrary points x and y. Then the norm $M(T - T')$ would start to decrease smoothly to zero as T is approaching T'. This point is illustrated in Fig. 1.4.

This analysis justifies to change the test space of differential m-forms for a test space in which the differential m-forms are more regular (i.e. whose variations are bounded). Until now we have considered the space of continuous differential forms which tend to zero at infinity (i.e. such that $\|\omega\|_\infty < \infty$). We would like to consider now differential forms which are differentiable and such that the derivatives are controlled: $\|\omega\|_\infty + \|\nabla\omega\|_\infty < \infty$. This leads naturally to define our test space as Sobolev spaces. Most of these spaces are Reproducible Kernel Hilbert Space (RKHS) as shown in Appendix B. Let W denote this new test space of differential forms. The associated space of currents is denoted W^*: the space of continuous mapping from W to $\mathbb{R}$. Then the mass-norm ($M(T) = \sup_{\|\omega\|_\infty \leq 1} |T(\omega)|$) is

replaced by the dual norm: $\|T\|_{W^*} = \sup_{\|\omega\|_W \leq 1} |T(\omega)|$. The kernel of the RKHS acts as a low-pass filter on the space of square integrable differential forms: this excludes from W the differential forms with too high frequencies (i.e. whose variations are not bounded).

Using RKHS as test space of differential m-forms have compelling advantages. First, the choice of the kernel determines how smooth the differential forms are. In particular, we can set a scale parameter which determines the rate of decay of the RKHS norm ($\|T - T'\|_{W^*}$) to zero when T is "converging" to T'. See Figure 3.16 for instance. If this scale tends to zero, then the RKHS norm tends to the mass-norm. For a larger parameter, shape dissimilarities are captured up to this scale. Second, in the framework of RKHS, the space of currents is provided with an inner-product and the norm, which is defined by a supremum, has a closed form. This makes the overall framework particularly well suited from a computational point of view. Third, the RKHS norm in the space of currents allows us to define random Gaussian variables. This will allow us to define statistical models of currents to measure the variability of shapes.

Remark 1.24 (Flat norm)**.** To workaround the bad behavior of the mass-norm, one introduces often the flat-norm defined as:

$$F(T) = \sup_{\|\omega\|_\infty \leq 1, \|d\omega\|_\infty \leq 1} |T(\omega)|\,, \tag{1.5.3}$$

where $d\omega$ denotes the exterior derivative of the differential m-form ω (see [Federer 1969, Cohen-Steiner 2003a], for instance). This norm introduces explicitly a control on the variations of the differential forms. However, by contrast to RKHS norm, this norm does not derive from an inner-product and has no closed form. This norm is therefore difficult to use from a computational point of view. □

1.5.2 The space of currents as the dual space of a RKHS

In this section, we adapt the construction of currents in Section 1.3 to a test space of differential forms which is a RKHS. We will show also how this framework enables to have a norm which derives from an inner-product and for which we have a closed-form.

For the sake of simplicity, we suppose, from now on, that we deal only with the practical cases of Section 1.4: sub-manifolds of dimension $0, 1, 2$ and 3 in $\mathbb{R}^3$ and sub-manifold of dimension $0, 1$ and 2 in $\mathbb{R}^2$. In all these cases, the differential m-forms can be seen as a scalar or vector field: a continuous mapping from $\mathbb{R}^d$ ($d = 2$ or $d = 3$) to $\mathbb{R}^p$ ($p = 0$ or $p = d$). The case $p = 0$ is for the scalar fields, the case $p = d$ is for the vector fields.

Note that the following construction could be made also for general differential m-forms (see Remark 1.28). However, this would involve more sophisticated notations without any benefits for the targeted applications.

1.5.2.1 A new space of currents

Let W be a Hilbert space of vector fields in which the vector fields are continuous and verifies:

$$\|\omega\|_\infty \leq C_W \|\omega\|_W \tag{1.5.4}$$

As shown in Appendix B, this condition makes W a RKHS (see Proposition B.4). From a numerical point of view, this condition implies that numerical error measured in the space W are numerically small.

We denote W^* the dual space of W, now our space of currents. The following proposition shows that the previous space of currents (i.e. the dual space of $\mathcal{C}^0(\mathbb{R}^d, (\Lambda^m\mathbb{R}^d)^*)$) is continuously embedded into W^*.

Proposition 1.25. *If T is a continuous linear form on $\mathcal{C}^0(\mathbb{R}^d, (\Lambda^m\mathbb{R}^d)^*)$ then it is a continuous linear form on W and*

$$\|T\|_{W^*} \leq C_W M(T). \tag{1.5.5}$$

Proof. By definition of a continuous linear map, we have that there is a constant C_T such that:

$$|T(\omega)| \leq C_T \|\omega\|_\infty , \tag{1.5.6}$$

which leads according to Eq. (1.5.4)

$$|T(\omega)| \leq C_T C_W \|\omega\|_W . \tag{1.5.7}$$

This shows that the T can be considered as current in W^*.

Moreover, we have:

$$\begin{aligned} \|T\|_{W^*} &= \sup_{\|\omega\|_W \leq 1} |T(\omega)| = \sup_{\|\omega\|_W \neq 0} \left| T\left(\frac{\omega}{\|\omega\|_W}\right)\right| \\ &\leq C_W \sup_{\|\omega\|_W \neq 0} \left| T\left(\frac{\omega}{\|\omega\|_\infty}\right)\right| \\ &\leq C_W \sup_{\|\omega\|_\infty \neq 0} \left| T\left(\frac{\omega}{\|\omega\|_\infty}\right)\right| = C_W M(T) \end{aligned} \tag{1.5.8}$$

■

This proposition shows that the RKHS norm on the space of currents is more precise than the mass-norm. It shows also that the currents introduced in the previous sections can be considered as currents in W^*. In particular, the Dirac delta currents as introduced in Definition 1.9 are currents in W^*. Proposition 1.4 which shows that a sub-manifold of $\mathbb{R}^d$ defines a current is still valid in this framework: under the same conditions sub-manifolds define a current in W^*. Indeed the inequality in Eq. (1.5.5) shows that a linear form on W which is continuous with respect to the $\|.\|_\infty$ norm is also continuous with respect to the W-norm. Proposition 1.11, which enables to approximate m-meshes T with finite sum of Dirac delta currents $\tilde{T}$, is also valid in W^*. Indeed, the proof relies on the inequality: $\left|T(\omega) - \tilde{T}(\omega)\right| \leq \varepsilon \|\omega\|_\infty$ for all $\omega \in \mathcal{C}^0(\mathbb{R}^d, (\Lambda^m\mathbb{R}^d)^*)$. This implies that for all $\omega \in W$, $\left|T(\omega) - \tilde{T}(\omega)\right| \leq \varepsilon C_W \|\omega\|_W$ and therefore that $\left\|T - \tilde{T}\right\|_{W^*} \leq \varepsilon C_W$ which tends to zero under the same conditions as in Proposition 1.11.

Eventually, the pull-back action on continuous differential m-forms (Definition A.11) extends straightforwardly to differential m-form in W under the same condition as in Definition A.11. Indeed, if ϕ is a diffeomorphism such that $\sup_{x\in\mathbb{R}^d} |d_x\phi| < \infty$, then

$|\phi^*\omega(x)| \leq \|\omega\|_\infty \|d_x\phi\|_\infty \leq C_{x,\phi} \|\omega\|_W$ which proves that the pullback vector field $\phi^*\omega$ belong to W. Therefore, we can define the push-forward action on currents as in Definition 1.15, which is now an action on the space of currents W^*.

1.5.2.2 Norm and inner-product in the RKHS

It is shown in Appendix B that there is an isometric mapping between the test space of vector/scalar field W and the space of current W^*. This mapping is denoted $\mathcal{L}_W$ and the kernel of the RKHS W is denoted K^W. This provides the space of currents W^* with a Hilbert structure. In this section, we show how this inner-product allows us to give a closed form to the norm $\|.\|_{W^*}$ in practical cases.

Proposition B.9 shows that the map $\mathcal{L}_W$ is isometric. Therefore the norm of a current $T \in W^*$ satisfies:

$$\|T\|_{W^*} = \sup_{\|\omega\|_W \leq 1} |T(\omega)| = \left\|\mathcal{L}_W^{-1}(T)\right\|_W , \tag{1.5.9}$$

and that the supremum is achieved for the vector field $\omega = \mathcal{L}_W^{-1}(T)$, which implies that $\|T\|_{W^*}^2 = T(\mathcal{L}_W^{-1}(T))$.

Now, we will show how to compute $\mathcal{L}_W^{-1}(T)$ and the norm of T when T is a sub-manifold or a finite set of Dirac delta currents. Assume first that T is a sub-manifold of $\mathbb{R}^3$ which can be seen as a current under the assumptions of Proposition 1.4 (assuming that the attribute map $I = 1$). We focus on the vectorial case (T is dimension 1 or 2) but the computations can be very easily adapted in the scalar case (T of dimension 0 or 3). Let $\omega \in W$ be a vector field, then by definition of $T(\omega)$ in Prop. 1.4 and thanks to the reproducing property in W (see Eq. (B.2.5)), we have:

$$\begin{aligned} T(\omega) &= \int_T \omega(x)^t \alpha(x) d\lambda(x) \\ &= \int_T \left\langle \omega, K^W(x,.)\alpha(x) \right\rangle_W d\lambda(x) \\ &= \left\langle \int_T K^W(x,.)\alpha(x) d\lambda(x), \omega \right\rangle_W \end{aligned} \tag{1.5.10}$$

where $\alpha(x)$ denotes the unit tangent of T at x if T is of dimension 1 or the unit normal of T at x if T is of dimension 2.

In section B.3 (Eq. (B.3.5)), it is shown that:

$$T(\omega) = \langle T, \mathcal{L}_W(\omega) \rangle_{W^*} \tag{1.5.11}$$

The combination of this equation with Eq. (1.5.10) shows that the mapping $\mathcal{L}_W^{-1}$ can be computed explicitly in this case as:

$$\mathcal{L}_W^{-1}(T)(x) = \int_T K^W(x,y)\alpha(y) d\lambda(y) \tag{1.5.12}$$

The representation of the sub-manifold in the space of vector fields W is given as the convolution between the kernel K^W and the dense field of its tangents or normals.

The application of the isometric mapping $\mathcal{L}_W$ (see Eq. (1.5.9)) leads to the norm of T as:

$$\begin{aligned}\|T\|^2_{W^*} &= \left\langle \mathcal{L}_W^{-1}(T), \mathcal{L}_W^{-1}(T) \right\rangle_W = \left\langle \int_T K^W(x,.)\alpha(x)d\lambda(x), \int_T K^W(x,.)\alpha(x)d\lambda(x) \right\rangle_W \\ &= \int_T \int_T \left\langle K^W(x,.)\alpha(x), K^W(y,.)\alpha(y) \right\rangle_W d\lambda(x)d\lambda(y) \\ &= \int_T \int_T \alpha(x)^t K^W(x,y)\alpha(y)d\lambda(x)d\lambda(y),\end{aligned} \tag{1.5.13}$$

by linearity of the integration and thanks to the reproducing property of the kernel (see Eq (B.2.5)).

Therefore, the Hilbert norm of the sub-manifold seen as a current is given by the double integration of the kernel on the manifold. Similar computations show that the inner-product between two sub-manifolds of the same dimension, T and T', is given by:

$$\langle T, T' \rangle_{W^*} = \int_T \int_{T'} \alpha'(y)^t K^W(y,x)\alpha(x)d\lambda(y)d\lambda(x), \tag{1.5.14}$$

where $\alpha(x)$ (resp. $\alpha'(x)$) denotes the tangent or normal of T (resp. T') at point x.

If the sub-manifold T is given as a m-mesh, it can be approximated, in the sense of Proposition 1.11 by a finite set of Dirac Delta currents: $T = \sum_{i=1}^n \delta_{x_i}^{\alpha_i}$. In this case, using Eq. (B.3.9), we have also explicit formulation for the representation of the current as a vector field:

$$\mathcal{L}_W^{-1}(T)(x) = \sum_{i=1}^n \mathcal{L}_W^{-1}(\delta_{x_i}^{\alpha_i})(x) = \sum_{i=1}^n K^W(x,x_i)\alpha_i, \tag{1.5.15}$$

also for the norm of this current:

$$\|T\|^2_{W^*} = T(\mathcal{L}_W^{-1}(T)) = \sum_{j=1}^n \delta_{x_j}^{\alpha_j}(\mathcal{L}_W^{-1}(T)) = \sum_{i=1}^n \sum_{j=1}^n \alpha_j^t K^W(x_j,x_i)\alpha_i \tag{1.5.16}$$

and the inner-product between T and $T' = \sum_{j=1}^m \delta_{y_j}^{\beta_j}$

$$\langle T, T' \rangle_{W^*} = \sum_{i=1}^n \sum_{j=1}^m \beta_j^t K^W(y_j,x_i)\alpha_i. \tag{1.5.17}$$

The comparison of these last two equations with Equations (1.5.13) and (1.5.14) shows that the approximation of Proposition 1.11 consists in replacing the continuous integrals by their Riemann sums. In other words, the continuous current T is decomposed into its *infinite* set of tangents or normals, whereas its discretization in the space of currents consists in sampling this field of tangents/normals. When the sampling becomes finer, the approximation converges in the space of currents. This shows that using RKHS enables to compare continuous objects with their discrete representation. This is a direct consequence of the construction of the RKHS as the completion of a pre-Hilbert space in the proof of Theorem B.6. This guarantees that the metric on currents is weakly sensitive to the sampling of the geometrical data, since each sampling is an approximation of the same continuous quantity. This ensures the robustness and numerical stability of this metric used in practical algorithms.

Table 1.2 summarizes these operations on currents for any m-currents in $3D$.

Remark 1.26. In this section we omit the scalar function I which can model attributes attached on the sub-manifold T. Taking into account such map induces only very slight changes in Eqs. (1.5.10) to (1.5.17). □

Remark 1.27 (Computational cost of the distance between currents)**.** In practice, we need mainly to compute the distance $\|T - T'\|_{W^*}$ between two set of Dirac Delta currents: $T = \sum_{i=1}^{N} \delta_{x_i}^{\alpha_i}$ (with N terms) and $T' = \sum_{j=1}^{N'} \delta_{x'_j}^{\alpha'_j}$ (with N' terms). For this purpose, one can use the equality: $\|T - T'\|_{W^*}^2 = \|T\|_{W^*}^2 + \|T'\|_{W^*}^2 - 2\langle T, T'\rangle_{W^*}$. Or one can form the current $S = \sum_{i=1}^{N+N'} \delta_{y_i}^{\beta_i}$ where $(y_i = x_i, \beta_i = \alpha_i)$ if $i = 1 \dots N$ and $(y_i = x'_i, \beta_i = -\alpha'_i)$ if $i = N{+}1, \dots, N{+}N'$ (i.e. the concatenation of the list of points (x,x') and the list of vectors $(\alpha,{-}\alpha')$) and compute directly $\|S\|_{W^*}$. The first solution requires to sum $N^2{+}(N')^2{+}NN'$ terms, whereas the second solution requires to sum $(N + N')^2 = N^2 + (N')^2 + 2NN'$ terms. The first solution is computationally less expensive than the second one. However, in chapter 2 we will present a computational framework which enables to compute these double sums at almost a constant cost, independently of the number of terms. This will make eventually the second solution about 3 times faster than the first one (3 double sums to be computed versus 1). □

1.5.2.3 Three norms on the space of currents

We can define 3 norms in the space of currents W^*. We introduced previously the mass-norm:

$$M(T) = \sup_{\|\omega\|_\infty \leq 1} |T(\omega)| \tag{1.5.18}$$

and the W^*-norm:

$$\|T\|_{W^*} = \sup_{\|\omega\|_W \leq 1} |T(\omega)|\,, \tag{1.5.19}$$

where T denotes a generic current in W^* and ω a generic scalar/vector field in W.

We saw that the mass norm generalizes the notion of volume of a m-dimensional sub-manifold and that this norm is not adapted to measure shape dissimilarity. The W^*-norm is a regularized version of the mass-norm which will allow us to drive the registration of shapes and define statistical models on shapes. Moreover, this norm is easily computable in practical cases.

In addition to these two norms, we can define the L^∞-norm of currents as:

$$\|T\|_\infty = \left\|\mathcal{L}_W^{-1}(T)\right\|_\infty, \tag{1.5.20}$$

where the norm on the right-hand side is the supremum norm of the scalar/vector field associated to the current T (this scalar/vector field belongs to W and therefore is continuous and tend to zero at infinity).

This last norm raises naturally when one considers the current T via the inner-products $\langle T, \delta_x^{\epsilon_k}\rangle_{W^*}$ for any points $x \in \mathbb{R}^d$ (ϵ_k denotes the canonical basis of $\mathbb{R}^3$ for vector fields and $\mathbb{R}$ for scalar field). Since $\langle T, \delta_x^{\alpha}\rangle_{W^*} = \mathcal{L}_W^{-1}(T)(x)^t\alpha$, we have the following property:

$$\|T\|_\infty = \sup_{|\alpha|=1, x\in\mathbb{R}^d} |\langle T, \delta_x^{\alpha}\rangle_{W^*}| \tag{1.5.21}$$

Norm on vector fields	Norm on currents	Comments
$\|\omega\|_\infty = \sup_{x\in\mathbb{R}^3} \|\omega(x)\|$	$M(T) = \sup_{\|\omega\|_\infty \leq 1} \|T(\omega)\|$	If T is a submanifold, $M(T)$ is the length, area, volume of T
$\|\omega\|_W$ (regularized L^2-metric)	$\|T\|_{W^*} = \sup_{\|\omega\|_W \leq 1} \|T(\omega)\|$	derives from an inner-product
	$\begin{aligned}\|T\|_\infty &= \left\|\mathcal{L}_W^{-1}(T)\right\|_\infty \\ &= \sup_{\substack{\|\alpha\|=1 \\ x\in\mathbb{R}^3}} \|\langle T, \delta_x^\alpha\rangle_{W^*}\|\end{aligned}$	corresponds to the weak-topology on W^*

Relations between norms:
$$\begin{aligned}&\|\omega\|_\infty \leq C_W \|\omega\|_W \\ &\|T\|_{W^*} \leq C_W M(T) \\ &\|T\|_\infty \leq \left(\sup_{x\in\mathbb{R}^3} \left|K^W(x,x)\right|\right) \|T\|_{W^*}\end{aligned}$$

Table 1.1: The norms on currents and vector fields

Since the span of the Dirac delta currents is dense in W^*, this equation shows that a sequence of currents T_n converges to 0 with respect to the L^∞-norm ($\|T_n\|_\infty \to 0$) if and only if $\langle T_n, T'\rangle_{W^*} \to 0$ for every currents $T' \in W^*$. This shows that the L^∞-norm is associated to the weak topology of the RKHS.

As a consequence, we can control the L^∞- by the W^*-norm. Indeed, we have:

$$|\langle T, \delta_x^\alpha\rangle_{W^*}| \leq \|T\|_{W^*} \|\delta_x^\alpha\|_{W^*} . \tag{1.5.22}$$

Moreover, $\|\delta_x^\alpha\|_{W^*}^2 = \alpha^t K^W(x,x)\alpha \leq \sup_{x\in\mathbb{R}^3} \left|K^W(x,x)\right| |\alpha|^2$ where $\left|K^W(x,x)\right|$ denotes the spectral norm of the matrix $K^W(x,x)$. Therefore, $\sup_{|\alpha|=1} |\langle T, \delta_x^\alpha\rangle_{W^*}| \leq \sup_{x\in\mathbb{R}^3} \left|K^W(x,x)\right|^{1/2} \|T\|_{W^*}$, which leads to:

$$\|T\|_\infty \leq \left(\sup_{x\in\mathbb{R}^3} \left|K^W(x,x)\right|^{1/2}\right) \|T\|_{W^*} \tag{1.5.23}$$

Both L^∞- and W^*-norm will be used in the next chapters, for instance to control the convergence of the matching pursuit in Chapter 3.

Remark 1.28 (RKHS of differential forms)**.** In this section, we provide the space of currents with a norm in the case of currents which can be represented by scalar or vector fields. This has been done for the sake of simplicity. We could have built also a RKHS of differential m-forms. The reproducing property would have been: $\omega(x)(u_1, \ldots, u_m) = \langle \omega, K(x,.)(u_1, \ldots, u_m)\rangle_W$ and the kernel K would have been a m-covariant, m-contravariant tensor. The construction would have been very similar to the one presented here. □

Remark 1.29 (Units)**.** The physical objects defined in this chapter (differential form, vector fields, currents, etc.) have dimension and therefore their measure depends on the choice of the unit of the ambient Euclidean space $\mathbb{R}^2$ or $\mathbb{R}^3$. The action of a m-form on a set

of m vectors leads to a real number which has no dimension and which is invariant under a change of coordinate. Since the vectors have the dimension of a length, denoted here L, a m-form is of dimension L^{-m}. A current integrates a m forms to give an adimensional real number: it is of dimension L^m. Therefore, it has the same dimension that the geometric object, which it models. The norm of the current $\|T\|_{W^*} = \sup_{\omega \neq 0} |T(\omega)| \, \|\omega\|$ has the dimension L^m, namely the dimension of a length for a 1-current and the dimension of a area for a 2-current. The map $\mathcal{L}_W$ from W to W^* depends also on the choice of units: it is of dimension $L^m/L^{-m} = L^{2m}$. The inverse map is implemented by the matrix $K^W(x, y)$ whose elements is of dimension L^{-2m}.

In Section 1.2 and 1.5 as well as in Appendix A, we identify differential 1-forms and vector fields, whereas the former is of dimension L^{-1} and the later of dimension L. Therefore, this identification depends on the choice of the units in the ambient Euclidean space: if the units change, the vector field associated to the 1-form also changes. This is well-known in differential geometry: the form is a covariant tensor, the vector field a contravariant tensor. One transforms the former into the later by applying the metric tensor, which is of dimension L^2. Therefore, these kind of identification can be made only once the units are fixed. In our applications, units are given by the imaging device. □

1.5.3 Random Gaussian Currents

Defining the test space W as a RKHS has another advantage: it allows us to define random Gaussian currents. Indeed, there is a standard way to define random Gaussian variables in infinite-dimensional Hibert spaces, so that their projection on any finite-dimensional subspace is a usual multi-variate Gaussian variable. In this setting, the kernel of a RKHS gives the covariance of the random variables. In this section, we show how such variables can be defined. In Section 2.3.3, we will show that the projection of the Gaussian currents on finite-dimensional spaces are usual Gaussian vectors.

First, we will show how the finite-dimensional case can be generalized to define infinite-dimensional random variables. Let Γ be a zero-mean Gaussian vector in $\mathbb{R}^n$ with covariance K. By definition, for any n-dimensional vector ω, $\omega^t \Gamma$ is a zero-mean Gaussian real variable with variance $\omega^t K \omega$. This shows that the covariance matrix K can be seen as a metric on $\mathbb{R}^n$. Actually, one can consider that the Gaussian variable Γ maps every eigenvectors $(e_i)_{i=1,\ldots,n}$ of K to an independent Gaussian real variables γ_i with variance given by the eigenvalues λ_i^2. Therefore, any vector ω is mapped into $\omega^t \Gamma = \sum_{i=1}^{n} \omega^t e_i \gamma_i$. This shows that a given metric K determines a Gaussian vector Γ. This idea of mapping each eigenvector of the metric to an independent Gaussian variable can be generalized in infinite-dimension as follows.

A current T is a linear mapping from a test space of vector field W (with metric K^W) to the space of real numbers $\mathbb{R}$. A random Gaussian current is a linear mapping from the test space W to a Gauss space $\mathcal{G}$[2]. This means that a random Gaussian current maps

[2] a Gauss space is a set of random Gaussian variables. The typical example of a Gauss space is the linear span of N independent Gaussian variables.

every vector field ω to a real random Gaussian variable $X^*(\omega)$, whereas a deterministic current maps the test vector field ω to a real number $T(\omega)$. We define this mapping such that the random current X^* tested on two *orthogonal* vector fields ω and ω' leads to two *independent* Gaussian variables. X^* can be seen as the Gaussian variable associated to the RKHS W with kernel K^W. However, since it is infinite-dimensional, it has no probability density function.

To give a precise definition, we assume that the test space W is separable. As such, W can be provided with an orthogonal basis w_n. We define the linear mapping X^* from W to $\mathcal{G}$ via its value on the orthogonal basis $(w_n)_{n=0,\dots,\infty}$: we set $X^*(w_n) = \gamma_n$, where γ_n is an infinite sequence of independent normal variables (zero mean and unit variance). Since every vector field ω can be decomposed into $\omega = \sum_{n=0}^{\infty} \langle \omega, w_n \rangle_W w_n$ such that $\|\omega\|_W^2 = \sum_{n=0}^{\infty} |\langle \omega, w_n \rangle_W|^2 < \infty$, we have by linearity of the mapping X^*: $X^*(\omega) = \sum_{n=0}^{\infty} \langle \omega, w_n \rangle_W \gamma_n$. Therefore for all $\omega \in W$:

$$\begin{aligned} &\mathbb{E}\left(X^*(\omega)\right) = 0 \\ &\mathbb{E}\left(X^*(\omega)^2\right) = \sum_{n=0}^{\infty} |\langle \omega, w_n \rangle_W|^2 = \|\omega\|_W^2 \end{aligned} \tag{1.5.24}$$

Moreover, given two vector fields ω and ω', we have:

$$\begin{aligned} \mathbb{E}\left(X^*(\omega)X^*(\omega')\right) &= \mathbb{E}\left(\left(\sum_{n=0}^{\infty} \langle \omega, w_n \rangle_W \gamma_n\right)\left(\sum_{m=0}^{\infty} \langle \omega, w_m \rangle_W \gamma_m\right)\right) \\ &= \sum_{n=0}^{\infty} \langle \omega, w_n \rangle_W \langle \omega', w_n \rangle_W = \langle \omega, \omega' \rangle_W . \end{aligned} \tag{1.5.25}$$

These intrinsic definitions of the variance and covariance of real variables $X^*(\omega)$ in Equations (1.5.24) and (1.5.25) shows that the definition of the random Gaussian current does not depend on the choice of the basis on W. This leads to the following definition:

Definition 1.30. *Let W be a separable Hilbert space of vector fields and $\mathcal{G}$ a Gaussian space. Let X^* be the isometric mapping between W and $\mathcal{G}$:*

$$\begin{array}{rccc} X^*: & W & \longrightarrow & \mathcal{G} \\ & \omega & & X^*(\omega) \end{array} \tag{1.5.26}$$

such that for all $\omega, \omega' \in W$:

$$\begin{aligned} &\mathbb{E}\left(X^*(\omega)\right) = 0 \\ &\mathbb{E}\left(X^*(\omega)X^*(\omega')\right) = \langle \omega, \omega' \rangle_W \end{aligned} \tag{1.5.27}$$

If the test space W is a RKHS, then we can test the Gaussian current on the basis vector $K^W(x,.)\alpha$. This leads to:

$$\mathbb{E}\left(X^*\left(K^W(x,.)\right)X^*\left(K^W(y,.)\beta\right)\right) = \alpha^t K^W(x,y)\beta. \tag{1.5.28}$$

This shows that the kernel determines the covariance of the random Gaussian currents. If the kernel is diagonal, in the sense $K(x,y) = 0$ if $x \neq y$, then the vectors $K(x,.)\alpha$ build an

orthogonal basis of the RKHS W. This is not the case in general but we can always build an orthogonal basis from these vectors via the Gram-Schmidt process.

This definition constructs theoretically a random Gaussian current with zero mean and a covariance structure determined by the kernel. However, in absence of probability function, there is no simple way to simulate some instances of this random current. In the next chapter, we will introduce finite-dimensional spaces to approximate the space of currents. The projections of this random current on these subspaces have a probability density function (pdf) as we will show in Section 2.3.3 and can be simulated numerically as we shall show and discuss in Section 3.5.

1.6 Conclusion

In this chapter, we gave a rather general presentation of currents. We discussed the ability of this framework to model a large range of geometrical objects, some with local orientation such as curves or surfaces, other without local orientation like point sets or volumes, some defined in the continuous domain, other defined as discrete structures, possibly provided with scalar attributes. Eventually, we provided the space of currents with a RKHS norm and inner-product. This offers a way to adapt the metric on currents to every particular anatomical data.

However, dealing with discrete currents, such as the ones resulting from the approximation in Proposition 1.11, may be computationally expensive, especially when the number of mesh cells increases, as mentioned in Remark 1.27. The following chapters are precisely dedicated to the design of an efficient numerical framework for currents.

From now on, we focus on the cases of curves and surfaces modeled as 1- and 2-currents, as the most interesting cases for our applications. For the sake of simplicity, we will use also 0-currents in some synthetic examples. We will use the scalar attributes to weight different parts of the currents as in Chapter 7, but we will not use such attributes for modeling non-geometrical properties of the shapes, according to Remark 1.14.

Dimension m	0-current	1-current	2-current	3-current
Differential m-form $x \to \omega(x)$	$a \in \mathbb{R} \to a\omega(x)$ scalar field	$\alpha \to \omega(x)^t \alpha$ vector field	$(\alpha, \beta) \to \omega(x)^t(\alpha \times \beta)$ vector field	$(\alpha, \beta, \gamma) \to$ $\det(\alpha, \beta, \gamma)\omega(x)$ scalar field
Sub-manifolds as continuous currents	set of points $\{x_1, \ldots, x_N\}$	param. curve $t \to L(t)$	param. surface $(u, v) \to S(u, v)$	Volume
Example of discrete currents	$\sum_i \delta_{x_i}^{a_i}$ a_i: scalars	$\sum_i \delta_{x_i}^{\alpha_i}$ α_i: vectors	$\sum_i \delta_{x_i}^{\alpha_i \times \beta_i}$ $\alpha_i \times \beta_i$: vectors	$\sum_i \delta_{x_i}^{v_i}$ $v_i = \det(\alpha_i, \beta_i, \gamma_i)$: scalars
Action on diff. forms (sub-manifolds)	$T(\omega) =$ $\sum_i a_i \omega(x_i)$	$T(\omega) =$ $\int_L \omega\left(L(t)\right)^t \frac{dL(t)}{dt} dt$	$T(\omega) =$ $\int_S \omega\left(S(u,v)\right)^t \left(\frac{\partial S}{\partial u} \times \frac{\partial S}{\partial v}\right) dudv$	$T(\omega) =$ $\int_V \omega(x) dx$
Action on diff. forms (discrete currents)	$\sum_i a_i \omega(x_i)$	$\sum_i \omega(x_i)^t \alpha_i$	$\sum_i \omega(x_i)^t (\alpha_i \times \beta_i)$	$\sum_i v_i \omega(x_i)$
Push-forward action	$\phi_* T(\omega) =$ $T(\omega \circ \phi)$	$\phi_* T(\omega) =$ $T(d_x\phi^t \omega \circ \phi)$	$\phi_* T(\omega) =$ $T\left(\lvert d_x\phi \rvert\, d_x\phi^{-1} \omega \circ \phi\right)$	$\phi_* T(\omega) =$ $T\left(\lvert d_x\phi \rvert\, \omega \circ \phi\right)$
Push-forward (discrete currents)	$\phi_*\left(\delta_x^a\right) = \delta_{\phi(x)}^a$	$\phi_*\left(\delta_x^\alpha\right) = \delta_{\phi(x)}^{d_x\phi(\alpha)}$	$\phi_*\left(\delta_x^{\alpha\times\beta}\right) = \delta_{\phi(x)}^{d_x\phi(\alpha)\times d_x\phi(\beta)}$ $= \delta_{\phi(x)}^{\lvert d_x\phi \rvert d_x\phi^{-t}(\alpha\times\beta)}$	$\phi_*\left(\delta_x^v\right)$ $= \delta_{\phi(x)}^{\lvert d_x\phi \rvert v}$
Inner-product btw sub-manifolds	$\sum_{i,j} a_i K(x_i, x_j) a_j$	$\iint_{L\times L'} \tau(t)^t K(L(t), L'(u)) \tau'(u) dtdu$ $\tau(t) = \frac{dL(t)}{dt} \quad \tau'(u) = \frac{dL'(u)}{du}$	$\iint_{S\times S'} n(x)^t K(S(x), S'(y)) n'(y) dxdy$ $n(x) = \frac{\partial S(x)}{\partial x_1} \times \frac{\partial S(x)}{\partial x_2}$ $n'(y) = \frac{\partial S'(y)}{dy_1} \times \frac{\partial S'(y)}{\partial y_2}$	$\iint_{V\times V'} K(x, y) dxdy$
Inner-product btw discrete currents	$\sum_{i,j} a_i K(x_i, x_j) a_j$	$\sum_{i,j} \tau_i^t K(x_i, y_j) \tau_j'$	$\sum_{i,j} n_i^t K(x_i, y_j) n_j'$	$\sum_{i,j} v_i K(x_i, y_j) v_j'$

Table 1.2: Summary of the operations on m-currents in $3D$, for $m = 0, \ldots, 3$